Science of the Total Environment 680 (2019) 151–168

Contents lists available at ScienceDirect

Science of the Total Environment

journal homepage: www.elsevier.com/locate/scitotenv

Assessing the provision of carbon-related ecosystem services across a range of temperate grassland systems in western Canada

Majid Iravani [a,b,*], Shannon R. White [a], Daniel R. Farr [c], Thomas J. Habib [a], Jahan Kariyeva [a], Monireh Faramarzi [b]

[a] Alberta Biodiversity Monitoring Institute, Department of Biological Sciences, University of Alberta, Edmonton, Alberta T6G 2E9, Canada
[b] Watershed Science and Modelling Laboratory, Department of Earth and Atmospheric Sciences, University of Alberta, Edmonton, Alberta T6G 2E3, Canada
[c] Environmental Monitoring and Science Division, Government of Alberta, Edmonton, Alberta T5J 5C6, Canada

HIGHLIGHTS

- A modeling framework was developed to improve simulation of carbon-related ES.
- Inaccurate results were obtained using prior knowledge or by partial model calibration.
- Robust simulation results were obtained using a regionalized parameterization scheme.
- A diverse range of climate change effects on grassland carbon-related ES was observed.
- Grazing management can be a climate change adaptation strategy in Alberta's grasslands.

GRAPHICAL ABSTRACT

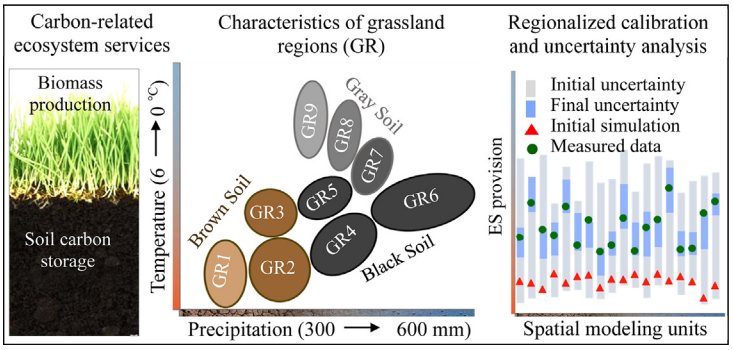

ARTICLE INFO

Article history:
Received 9 January 2019
Received in revised form 7 May 2019
Accepted 7 May 2019
Available online 09 May 2019

Editor: Paulo Pereira

Keywords:
Biogeochemical processes
Calibration and uncertainty
Climate change
Grazing management
Plant biomass production
Soil carbon stock

ABSTRACT

Reliable data on the provision of ecosystem services (ES) is essential to the design and implementation of policies that incorporate ES into grassland conservation and restoration. We developed and applied an innovative approach for regional parameterization, and calibration of the CENTURY ecosystem model. We quantified spatiotemporal variation of soil organic carbon stock (SOC) and aboveground plant biomass production (AGB) and examined their responses to the recent climate change across a diverse range of native grassland systems in Alberta, western Canada. The simultaneous integration of SOC and AGB into calibration and analysis accounted for most of the spatiotemporal variability in the SOC and AGB measurements and resulted in reduced simulation uncertainty across nine grassland regions. These findings suggest the importance of the systematic parameterization and calibration for the reliable assessment of carbon-related ES across a wide geographic area with heterogeneous ecological conditions. Simulation results showed a pronounced variation in the spatial distribution of SOC and AGB and their associated uncertainty across grassland regions. Under baseline grazing intensity regime, an overall negative effect of recent climatic changes on the SOC, and a less consistent effect on the AGB were found. While, an overall positive or slightly negative impact of recent climate change on the SOC and AGB was found under a proposed 10% lower grazing intensity regime. These heterogeneities in the magnitude and direction of climate change effects under different grazing regimes suggest needs for a range of climate change adaptation strategies to maintain carbon-related ES in Alberta's grasslands. The modeling framework developed in this study can be used to improve the spatially explicit assessment of carbon-related ES in other geographically vast grassland areas and examine the effectiveness of alternative management scenarios to ensure the long-term provision of carbon-related ES in grassland systems.

* Corresponding author.
E-mail address: iravani@ualberta.ca (M. Iravani).

https://doi.org/10.1016/j.scitotenv.2019.05.083
0048-9697/

1. Introduction

Grasslands are one of the earth's major biomes that cover >40% of the earth's terrestrial surface (Hewins et al., 2018). They occur under a broad range of climatic, topographic and edaphic conditions and support a diverse assemblage of plant and animal communities (Blair et al., 2014). Grasslands play a major role in local, regional and global biogeochemical cycles by storing vast amounts of carbon and critical nutrients in their soils (Parton et al., 1988; Hungate et al., 2017). They provide a host of critical ecosystem services (ES), including carbon stock for climate regulation, forage production for wildlife and livestock grazing, pollination services for adjacent crop fields, clean water for human consumption among others (Gibson, 2009; Blair et al., 2014). However, several of these environmental, economic and socio-cultural services are undervalued as indicated by limited policies to promote ES conservation and restoration in grassland systems (Havstad et al., 2007; Jellinek et al., 2019).

Carbon-related ES provided through organic carbon stock in soil and aboveground plant biomass production are critical services that ensure the provision of several other ES (Adhikari and Hartemink, 2016; Hungate et al., 2017). Recently, carbon-related ES have been used as the basis for innovative approaches to incentivize grassland conservation and restoration activities such as issuing credits for land management practices that encourage carbon stock in grassland soil (Havstad et al., 2007; Jack et al., 2008; Jellinek et al., 2019). Robust, reliable and comparable data on the provision of carbon-related ES and the potential trade-off among those services are necessary to design and implement policies that incorporate ES valuation in grassland conservation and restoration (Daily et al., 2009; Cord et al., 2017). However, for most geographic regions, spatially explicit and comprehensive data on the provision of carbon-related ES are lacking (Howe et al., 2014; Schulp et al., 2014).

Application of the biogeochemical ecosystem models are among the best available means to account for the provision of carbon-related ES at large spatial scales (e.g., Lugato et al., 2014; Campbell and Paustian, 2015; Dimassi et al., 2018; Sándor et al., 2018). The process-based models are generally highly complex and comprise numerous biophysical and empirical parameters associated with the simulation of various ecosystem processes. These input parameters are not measurable and they require proper parameterization and calibration to ensure that target ecosystem processes are adequately represented (Cuddington et al., 2013; Necpálová et al., 2015). The process-based models are typically calibrated manually through a "trial and error" approach, where the most sensitive parameters for targeted processes are adjusted one-at-a-time, iteratively in multiple stages, until simulated and measured values are matched reasonably well (Brandani et al., 2015; Lugato et al., 2014). However, due to nonlinear behavior of the underlying interactions among model parameters and corresponding physical processes, this approach does not necessarily yield optimal parameter estimates for simulated ecosystem processes (Rafique et al., 2013; Faramarzi et al., 2015; Rafique et al., 2015).

Inverse modeling approaches that employ algorithmic parameter estimation techniques have been widely used in recent years to parameterize and calibrate process-based models (Niquil et al., 2011; Meersmans et al., 2013; Kwon et al., 2017). These algorithms employ mathematical and statistical procedures along with empirically measured data to enable more reliable estimates of model parameters and outputs by providing valuable insight about model functions and their underlying ecosystem processes (Necpálová et al., 2015; Rafique et al., 2015). However, the main concern with inverse modeling is the issue of non-uniqueness, where numerous input parameter sets can reproduce the desirable output (i.e., there will be many 'best' solutions rather than only one; Faramarzi et al., 2015). With the recent advancements in inverse modeling techniques, the issue of non-uniqueness can be represented by parameter uncertainty prediction (Faramarzi et al., 2017). In addition, inverse modeling facilitates the assessment of uncertainty sourcing from input data, model algorithm and lack of process representation in the model structure (Kwon et al., 2017). This is crucial because geo-referenced, consistently measured, and harmonized field data for large-scale modeling are generally limited (Schulp et al., 2014; Cuddington et al., 2013) and direct measurement of model parameters describing various ecosystem processes is time intensive, expensive and often has limited applicability (Abbaspour et al., 2007).

As the end-product of various interrelated biophysical processes, the spatiotemporal patterns of grassland ES provision significantly vary among carbon-related ES (Parton et al., 1987; Parton et al., 1993; Schimel et al., 1994; Brown et al., 2010; Howe et al., 2014; de Gruijter et al., 2016; Wiesmeier et al., 2019). Also, there is significant uncertainty about the biophysical production of carbon-related ES under varying ecological conditions in grasslands (Ogle et al., 2007; Van den Bygaart et al., 2008; Xiong et al., 2015). Moreover, spatiotemporal variability in climate in combination with land use practices (e.g., grazing) increase uncertainty predictions for future adaption and grassland management actions. This spatiotemporal variability makes carbon-related ES challenging to reliably estimate using biogeochemical ecosystem models, particularly over a large geographic area with substantial uncertainty associated to input data among others (Cerri et al., 2007; Ogle et al., 2010; Oelbermann and Voroney, 2011; Hou et al., 2013; Lugato et al., 2014).

The inverse modeling approach and the advancements in quantifying simulation uncertainties proved to be useful in various process-based eco-hydrogeological models (Abbaspour et al., 2007; Niquil et al., 2011; Faramarzi et al., 2015). Nevertheless, the approach has been rarely applied to parameterize and calibrate complex ecosystem models with the aim of assessing the provision of carbon-related ES in grasslands (Rafique et al., 2013; Necpálová et al., 2015; Rafique et al., 2015; Kwon et al., 2017). To our knowledge, no previous study has demonstrated the full use of inverse modeling approach to rigorously assess carbon-related ES and their associated uncertainties across a range of ecological conditions in grassland systems. The partial accounting of the carbon-related ES in traditional approaches and lack of quality and quantity data limit the level of confidence in using the simulation results to inform management decisions in grasslands (Daily et al., 2009; Schulp et al., 2014).

We performed a comprehensive parameterization and calibration of the CENTURY ecosystem model (Parton et al., 1988) across a wide range of grassland regions in Alberta, a western province of Canada. We hypothesized that a regionalized parameterization scheme and the use of two types of spatially and temporally different field measurements on carbon-related ES could help a satisfactory simulation of soil organic carbon stock (SOC) and aboveground plant biomass production (AGB) across Alberta's native grasslands. More specifically, our objectives were to: (i) test a single-variable versus a multi-variable calibration approach in assessing the spatially explicit simulation of the SOC and AGB and their potential trade-offs; (ii) assess the level of precision and uncertainty in simulation of the SOC and AGB across a range of ecological conditions; (iii) examine the impacts of recent climate change on the SOC and AGB and (iv) assess whether grazing management can serve as a potential adaptation strategy to maintain the SOC and ABG in highly valued native grasslands of Alberta.

2. Material and methods

2.1. Description of the study area

Alberta, with an area about 661,190 km^2, is one of the westernmost and largest provinces of Canada (49–60°N and 110–120°W; Fig. 1). It extends for approximately 1223 km from north to south with about 660 km wide (at its greatest east-west extent) and varies in altitude from 152 to 3747 m (Stamp and Warnell, 2008). This, together with large-scale climate influences originating from the Pacific Ocean, has a pronounced influence on climate and ecological diversity (Lapp et al.,

2013). In general, the northern and western parts of the province experience greater rainfall, while the south and east-central portions are prone to drought-like conditions sometimes continuing for several years. The average annual precipitation ranges from 300 mm in the southeast to about 450 mm in the north and 600 mm in the foothills of the Rocky Mountains. The four months of May, June, July and August provide about double the precipitation amount compared to the other eight months of the year. The mean daily temperature in January ranges from −8 °C in the south to −24 °C in the north, whereas in July it ranges from 20 °C in the south to 16 °C in the north (Stamp and Warnell, 2008). Alberta is a sunny province (on average about 1900–2300 h sunshine per year; Stamp and Warnell, 2008) but Arctic air masses in the winter can produce extreme minimum temperatures varying from −54 °C in the north to −46 °C in the south. However, in the summer, continental air masses produce maximum temperatures ranging from 32 °C in the mountains and north to over 40 °C in the southern Alberta (Chetner and the Agroclimatic Atlas Working Group, 2003).

Alberta's native grasslands, with an area of about 6.5 million ha, are distributed across distinct natural regions with different climate, soil and vegetation types (Downing and Pettapiece, 2006). Most of the northern half of the province is boreal and Mixedwood forests. The southern quarter of the province is native prairie grasslands, ranging from shortgrass prairie in the southeastern corner to Mixedgrass and Fescue prairie grassland in an arc to the west and north of it. The Aspen Parkland region extends in a broad arc between the prairies and the boreal forests and the Foothills divide the conifer-dominated vegetation of the Rocky Mountains and the boreal uplands from the Aspen Parklands (Downing and Pettapiece, 2006). Most of the unforested part of the province is converted to annual crops and perennial forages, while ranching predominates in the south (Stamp and Warnell, 2008). Alberta has diverse soils that are strongly associated with variation in climate, vegetation and parent materials (Fig. 1). The dominant reference soil groups in native grassland areas are Chernozemic and Luvisolic soils (ASIC, 2001). Brown Chernozemic soils are found in the Southeast part give way to Dark Brown, Black and Dark Gray Chernozemic soils as one proceeds in a northwesterly direction. Gray Luvisols are found in boreal Mixedwood forests, and foothills of the Rocky Mountains (Chetner and the Agroclimatic Atlas Working Group, 2003). The brown Chernozemic soils are the least productive, while the Black Chernozemic soils are the most productive that are used to grow a wide variety of agricultural and forage crops (Downing and Pettapiece, 2006).

2.2. CENTURY ecosystem model

We used the plant-soil ecosystem model, CENTURY (v. 4.6; Parton et al., 1988; Parton et al., 1989), to simulate SOC and AGB. The CENTURY model has been identified as one of the most used models among the existing organic carbon models (Campbell and Paustian, 2015). It was initially developed for northern grasslands based on experiments in Great Plains (Parton et al., 1987), of which Alberta's native grasslands are a northern extension. The CENTURY model consists of several interactive sub-models to track organic carbon sequestration and stock in both grassland soil and plant biomass (Parton et al., 1988), thus it can estimate the provision of carbon-related ES in grasslands. This model has been used to simulate SOC (e.g., Parton et al., 1995; Gilmanov et al., 1997; Parton et al., 2004; Cerri et al., 2007; Álvaro-Fuentes et al., 2012; Lugato et al., 2014; Brandani et al., 2015) and AGB (e.g., Parton et al., 1993; Wang et al., 2008; Feng and Zhao, 2011; Lopez-Marsico et al., 2015; Kwon et al., 2017) across different terrestrial biomes and ecoregions, including Canadian Prairies (e.g., Smith et al., 1997b; Van den Bygaart et al., 2008; Smith et al., 2009; Oelbermann and Voroney, 2011), but often covering small areas or site-specific studies over large areas.

The CENTURY model uses empirically derived mathematical relationships to simulate biophysical processes involved in carbon and nutrient dynamics within the top ~20 - ~30 cm of the soil profile and at a monthly time step (Parton et al., 1988; Parton et al., 1989). It consists of several interconnected sub-models including soil organic matter and plant growth. The soil organic matter sub-model contains a surface microbial pool associated with decomposing surface litter, two aboveground litter pools (i.e., metabolic: readily decomposable and structural: resistant to decay), and three SOC pools representing a gradient in decomposability (i.e., active or microbial biomass and associated

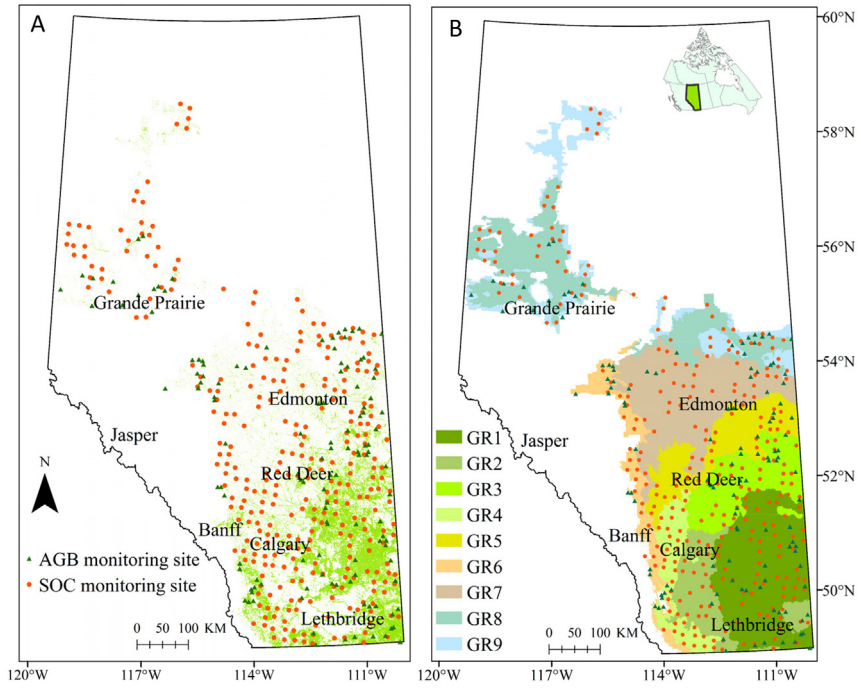

Fig. 1. Distribution of native grassland areas (A) and associated regions (B) together with the location of AGB and SOC measurement sites across the province of Alberta.

metabolites over months to years, slow over decades, passive over centuries). The sub-model distributes the nongaseous products, formed by microbially mediated decomposition of plant and soil organic residues, into either or both the surface microbial pool and the three SOC pools. The plant growth sub-model simulates plant growth and net primary production based on vegetation type, temperature, moisture and nutrient availability. It regulates the type and timing of the net primary production that is allocated to different litter and SOC pools (Parton et al., 1988). Primary input variables for the CENTURY model are monthly climate data (e.g., rainfall and minimum and maximum temperature), soil properties (e.g., soil texture, depth, bulk density, drainage class and pH), atmospheric and soil nitrogen inputs, lignin content of plant material and land management information (e.g., grazing and fire). Additional details on the model structure and data are given in Parton et al. (1987), Parton et al. (1988) and Parton et al. (1989).

2.3. Input data and initial model set up

We used the Agricultural Region of Alberta Soil Inventory Database (AGRASID v. 3.0) to obtain the necessary soil parameters for Alberta's native grasslands. The AGRASID represents the spatial distribution of about 2100 soil types within the agricultural extent of Alberta and includes >28,000 polygons with unique values for soil properties at a scale of 1:100000 (ASIC, 2001). We extracted soil polygons associated with native grassland areas (Fig. 1), as determined from the Alberta Biodiversity Monitoring Institute's (ABMI) Wall to Wall Land cover (v 1.0; ABMI, 2012) and Human Footprint maps (v 1.1; ABMI, 2016b). This resulted in 24,731 soil polygons comprising 658 soil types associated with nine distinct grassland regions with homogeneous vegetation types and climate conditions (Fig. 1, Table 1). These soil polygons served as the spatial units and represented in the CENTURY model (Fig. 2). For each spatial unit, we extracted soil properties (texture, bulk density, rock content and pH for 0–20 cm depth) and soil layers (depth and drainage class) from the AGRASID. Historical climate data (1901–2010) were extracted from ClimateWNA (Wang et al., 2012), which provides gridded (approx. 4 × 4 km) monthly climate data for Western North America based on interpolated historical weather station records. To initially set up the model, we used available literature to define rates for atmospheric nitrogen deposition (Alberta Environment, 2006), biological nitrogen fixation (Cleveland et al., 1999) and the carbon-to-nitrogen ratio (C/N) in litter and mineral soil (Smith et al., 1997b; Murphy et al., 2002). We set initial parameter values for Alberta's grasslands, through consultations with the CENTURY Core Group at Colorado State University. All other model parameters were left to default values or in the case of initial soil organic matter, established through equilibrium.

We initially ran the CENTURY model (from now on referred to as "initial simulation") with the coupled C—N sub-models (i.e., simulating nitrogen besides carbon) for three periods. First, we ran a 4900-year period (3000 BCE to 1900 CE) to reach equilibrium levels (i.e., initial conditions) of AGB and SOC under a natural disturbance regime (Parton et al., 1988), specified as fire event every six years and a two-month bison grazing event (i.e., shifting annually by two months) occurred every year (Wang et al., 2014). For this period, we used long-term (1901–2010) monthly climate averages (Parton et al., 1988; Oelbermann and Voroney, 2011; Brandani et al., 2015). Next, we ran a 60-year period (1901–1960) followed by a 50-year period (1961–2010) using actual monthly weather records. For these two last periods, we replaced bison grazing with cattle grazing during June–September with high (70% of shoots removed by grazing) and moderate grazing intensity (50% of shoots removed by grazing), respectively (Wang et al., 2014). Cattle grazing was represented using a quadratic impact on aboveground production and a linear impact on the root/shoot ratio as incorporated in the CENTURY model (Holland et al., 1992). We also removed fire events from these two last periods as fire has been suppressed mainly in Alberta since European settlement (Wang et al., 2014).

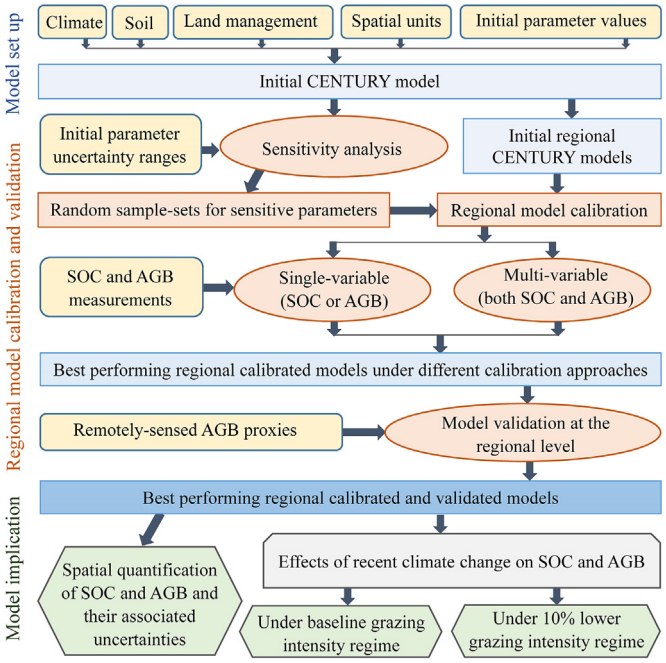

Fig. 2. A schematic diagram of the various modeling tasks and data analysis employed.

2.4. Model calibration and validation

2.4.1. Measured data

Three different types of measured data were used for model calibration and validation analysis (Fig. 2). We used measured SOC and AGB data for model calibration and remotely sensed AGB proxies for model validation at the regional level. A brief description of each data set is provided as follow:

Table 1
Characteristics of nine regions defined for native grasslands of Alberta. Regions are ordered based on their geographic locations (Fig. 1).

Region	Description	Area (km^2)	Precipitation (mm)	Temperature (°C)	No. soil types	No. spatial units
GR1	Brown soil of Dry Mixedgrass	23,316.8	344	4.8	77	4958
GR2	Dark Brown soil of Mixedgrass	5547.7	406	4.9	79	2196
GR3	Dark Brown soil of Northern Fescue	7359.6	400	3.4	40	2908
GR4	Black soil of Foothills Fescue	3694.8	467	4.3	50	1815
GR5	Black soil of Central Parkland	2496.4	454	3.0	49	2501
GR6	Black soil of Foothills Parkland	2458.4	569	3.2	65	2098
GR7	Black-Dark Gray soil of Parkland & Mixedwood	2335.9	482	2.7	101	4198
GR8	Dark Gray-Black soil of Mixedwood & Parkland	951.3	466	2.1	104	2400
GR9	Gray-Dark Gray soil of Mixedwood	794.6	459	1.6	115	1657

Measured SOC data: Through its ongoing monitoring program, the ABMI has measured (2007–2017) SOC in the top mineral soil layer (four pooled soil samples from 0 to 5 cm depth) at approximately 330 grassland monitoring sites systematically spaced throughout native grasslands of the province (ABMI, 2016a; Fig. 1). Because the CENTURY model simulates SOC at a depth of 0–20 cm, we extrapolate ABMI's 0–5 cm SOC measurements to about 0–20 cm using SOC data reported in the AGRASID. We extracted SOC data for native grassland soil types (Table 1) with at least three SOC records in the first 30 cm depth of mineral soil (391 soil types, 1216 mineral soil layers with variable thickness). For each region (Fig. 1), we then employed a bootstrap resampling procedure (R v. 3.1.1 and *resample* package; R Development Core Team, 2017) with a resampling size of at least 30 and established the best-fit regression line for the depth distribution of SOC using the curves and their associated confidence intervals generated from the resampled datasets (Fig. A1). We then used regional conversion factors derived from the established regression models (fitted SOC values at 5 and 20 cm depths) to extrapolate ABMI's SOC measurements to the first 20 cm depth of grassland soil. The constructed dataset for SOC measurements was used for our model calibration analysis.

Measured AGB data: The Range Resource Program of Alberta Environment and Parks (AEP) has completed long-term AGB measurements at >100 Rangeland Reference Areas spaced throughout native grasslands of the province (AESRD, 2015; Fig. 1). At the beginning of each growing season, ten cages (each 1.5 m × 1.5 m) were placed at each rangeland site (moved annually) and then vegetation within each cage was clipped to the ground level at the end of the growing season (late August, September). The average AGB in each site was then calculated based on the dry weight of live plant materials clipped from the temporary cages (AESRD, 2015). For this study, we had access to time series of AGB measurements from 93 rangeland sites that date back from the 1980s to 2000s, mostly to 1990s. The constructed dataset for AGB measurements was used for our model calibration analysis.

Remotely sensed AGB proxies: The integrated growing season vegetation greenness data derived from time-series of remotely sensed Normalized Difference Vegetation Index (NDVI) had been frequently used as a proxy of AGB in grasslands (e.g., Grigera et al., 2007; Gu et al., 2013; Gu and Wylie, 2015; Cord et al., 2017; Liu et al., 2017). We obtained the 16-day composite MODIS (Moderate Resolution Imaging Spectroradiometer) NDVI time series (250-m spatial resolutions) for the entire growing seasons of 2000–2010 period from the Land Processes Distributed Active Archive Center (Didan, 2015). We then employed TIMESAT time-series analysis software (Jönsson and Eklundh, 2004) to derive pixel-per-pixel proxy measures of annual AGB (2000 to 2010) which were then aggregated across the soil types within each grassland region (Table 1) for model validation. The TIMESAT software applies a number of time-series fitting algorithms and a range of threshold and parameter settings to derive several phenological metrics from the NDVI time series data including AGB proxy metrics based on the greenness (NDVI) values integrated over the complete growing season (i.e., the area under the seasonal growth curve). More details on the TIMESAT software are provided by Jönsson and Eklundh (2004), and Kariyeva and van Leeuwen (2012). The constructed dataset for remotely sensed AGB proxies was used for our model validation at the regional level.

2.4.2. Model calibration set up

We used Sequential Uncertainty Fitting (SUFI-2) algorithm for model calibration through an inverse modeling approach (Abbaspour et al., 2007; Faramarzi et al., 2015). The SUFI-2 combines calibration and uncertainty analyses and maps all sources of uncertainty (e.g., input data, model parameters, model structure and measured data) onto the parameter ranges. Different combinations of the parameter values can lead to a similar model simulation and therefore the solution may not be unique (Wang et al., 2013). However, since an accepted physically and biologically meaningful range is assigned to each input parameter, the optimized parameter ranges represent the narrowest uncertainty ranges that produce the best fit of the model simulations to the measurements (Necpálová et al., 2015). In SUFI-2, parameter uncertainty is described by a multivariate uniform distribution in a parameter hypercube, while the output uncertainty is quantified by the 95% prediction uncertainty band (95PPU) calculated at the 2.5% and 97.5% levels of the cumulative distribution function of the output variables. The algorithm starts with a large parameter uncertainty range (PUR) so that the measured data initially fall within the 95PPU. It then employs one or more types of objective functions (i.e., the measure of the numerical proximity of the simulated and measured data) allowing users to narrow down the PUR through iterative steps until a satisfactory model and calibration results are obtained (i.e., bracketing most of the measured data within the 95PPU while seeking the smallest possible uncertainty band). The strength of a calibration and uncertainty analysis is assessed using two indices: (i) the *p-factor* or the percentage of measured data bracketed by 95PPU (ranges between 0 and 1; with an ideal value of 1), and (ii) the *r-factor* or the average thickness of the 95PPU band divided by the standard deviation of the measured data (ranges between 0 and infinity; a practical value around 1 is suggested). More details on the SUFI-2 algorithm are provided by Abbaspour et al. (2007), Faramarzi et al. (2015) and Faramarzi et al. (2017).

We used available literature (e.g., Parton et al., 1989; Metherell et al., 1993; Gilmanov et al., 1997; Smith et al., 1997b; Murphy et al., 2002; Necpálová et al., 2015; Rafique et al., 2015; Sándor et al., 2018) to develop a general list of potentially sensitive input parameters for organic carbon dynamics in grasslands (Table 1 in Table A1) and to assign each of them a wide relevant PUR (i.e., physically and biologically meaningful minimum and maximum values). Next, we performed a one-at-a-time sensitivity analysis to come up with an initial list of potentially sensitive parameters to SOC and AGB and a reasonable PUR for the selected parameters (Abbaspour et al., 2007; Faramarzi et al., 2017). Further, we performed a global sensitivity analysis (Necpálová et al., 2015; Rafique et al., 2015) to screen and determine the most sensitive parameters to SOC and AGB and also to consider possible interactions among the selected parameters (Wang et al., 2013; (Fig. 2)). For global sensitivity analysis, we performed 500 model runs using the input parameter set-samples generated through a Latin Hypercube Sampling (LHS) procedure (R v. 3.1.1 and *spartan* package) that uses a stratification strategy to extract random samples from the entire PUR (Gupta et al., 1998; Abbaspour et al., 2007; Faramarzi et al., 2015). For a cost-effective simulation at this level of area coverage and spatial resolution, we parallelized our simulations in a 48-core advanced computing system. We then regressed the LHS generated parameter sets against the corresponding simulated SOC and AGB using a stepwise regression sensitivity analysis (R v. 3.1.1 and *MASS* package) to determine which of the tested parameters are sensitive to either or both SOC and AGB across Alberta's grasslands (Faramarzi et al., 2017).

To account for spatial variations in climate, soil and vegetation across Alberta's native grasslands, we performed regional (Table 1) parameterization and calibration of the CENTURY model using two different calibration approaches (Fig. 2). First, we performed a single-variable calibration approach where either SOC or AGB measurements were integrated into the calibration analysis (i.e., "SOC" calibration approach and "AGB" calibration approach, respectively). We implemented this approach to assess if partial calibration of the model against SOC or AGB measurements alone can provide reliable estimates for both SOC and AGB across different regions. We then performed a multi-variable calibration approach where both SOC and AGB measurements were integrated simultaneously into the calibration analysis (i.e., "Both" calibration approach). We implement this approach to determine if incorporating both types of spatially and temporally different field measurements (Fig. 1, Table 1) into a calibration scheme can improve model performance and reduce simulation uncertainty for both SOC and AGB across regions.

For each calibration approach, we performed multiple model runs (i.e., 500 simulations for each iteration) using the parameter set-samples generated through an LHS for the sensitive parameters. For each region, we then evaluated simulation results of the spatial units with measured data using two numerical criteria of PBIAS and RSR (i.e., objective functions), which are among the most recommended performance criteria for model calibration (Gupta et al., 1998 and its citations). The PBIAS, expressed as a percentage, is a measure of the deviation of simulation results from their measured counterparts. The RSR is a measure of the ratio of the standard deviation of the prediction errors (RMSE) to the standard deviation (SD) of measured values. Therefore, both PBIAS and RSR can indicate poor model performance. The optimal value of PBIAS is 0.0, with low-magnitude values indicating accurate model simulation. RSR varies from the optimal value of 0 to a large positive value. The lower the RSR, the lower the RMSE and the better the model simulation performance (Gupta et al., 1998; Abbaspour et al., 2007; Faramarzi et al., 2017). We calculated PBIAS and RSR using Eq. (1) and Eq. (2):

$$PBIAS = 100 \times \frac{\sum_{i=1}^{n} (Q_m - Q_s)_i}{\sum_{i=1}^{n} (Q_{m,i})} \quad (1)$$

$$RSR = \frac{\sqrt{\sum_{i=1}^{n} (Q_m - Q_s)_i^2}}{\sqrt{\sum_{i=1}^{n} \left(Q_{m,i} - \overline{Q}_m\right)^2}} \quad (2)$$

where, Q is a variable (i.e., SOC or AGB), m and s stand for measured and simulated values, respectively and i is the i^{th} measured or simulated data (Abbaspour et al., 2007). We assigned equal weight to both variables in multi-variable calibration approach (Faramarzi et al., 2017). Our regional parameterization, calibration and uncertainty schemes required a number of iterations to reach a desirable model performance under different calibration approaches.

2.4.3. Model validation at the regional level

The best performing calibrated models under different calibration approaches were used to perform model validation at the regional level. We compared the remotely sensed AGB proxies for the 2000–2010 period and the simulated AGB time series obtained through different calibration approaches (i.e., "SOC", "AGB" and "Both" calibration approach). The simulated AGB time series were based on regional optimized PUR and 500 model runs per approach for each spatial unit within each grassland region (Table 1). The performance assessment of the models for the validation period was based on comparing the simulated AGB with the corresponding time series of remotely sensed AGB proxies. For each model run, we conducted a Pearson's correlation analysis by pairing the data at the identical time points and replicating the spatial units (R v. 3.1.1). Further, we compared the aggregated Pearson's correlation coefficients of the nine grassland regions (500 correlation coefficient per region) to evaluate the performance of the three different calibration approaches across regions (Fig. 2).

2.5. Spatial quantification and uncertainty in SOC and AGB simulation

The best performing calibrated and validated model was used to quantify spatiotemporal variability of the SOC and AGB for the 2000–2010 period across Alberta's native grasslands (Fig. 2). First, we employed the regional optimized PUR determined through the multi-variable calibration approach to obtain time series of simulated SOC and AGB (annual values for the 2000–2010 period) for 500 simulations across all spatial units. For each spatial unit, we then obtained median values for SOC and AGB from the associated 95PPU bands of 500 simulations (i.e., output from the SUFI-2 algorithm) at a yearly time step (2000–2010 period). We then averaged the annual median values (i.e., M95PPU) obtained for each spatial unit to illustrate the spatial distribution of SOC and AGB across Alberta's native grasslands. In addition, for each spatial unit, we calculated the ratio of the 95PPU thickness (the difference between the upper and the lower limits) to the M95PPU at a yearly time step (2000–2010 period). We then averaged the annual ratios obtained for each spatial unit to illustrate spatial distribution of the uncertainty prediction in SOC and AGB across Alberta's native grasslands.

2.6. Recent climate change and its effects on SOC and AGB

We examined the change in annual precipitation and minimum and maximum temperature between two 20-year periods of the 1970s (1961–1980) and the 2000s (1991–2010) using historical climate data (ClimateWNA; Wang et al., 2012). We then used area-weighted average changes in precipitation and temperature at the township scale to illustrate spatial patterns of recent climatic changes across Alberta's native grasslands.

We used the best performing calibrated and validated model to assess the effects of recent climatic changes on SOC and AGB across Alberta's native grasslands. We examined the change in SOC and AGB between two 20-year periods of the 1970s (1961–1980) and the 2000s (1991–2010). To assess the effectiveness of grazing management as a potential climate change adaptation strategy, we assessed the change in SOC and AGB between these two periods under baseline grazing intensity regime and a 10% lower grazing intensity regime (Fig. 2). The baseline grazing intensity regime was represented by the optimized PUR for the fraction of plant biomass removed by grazing (*flgrem* parameter) under the multi-variable calibration approach (Table A2). The 10% lower grazing intensity was proposed based on personal communications with the beef producers in Alberta.

For the baseline grazing intensity regime, we obtained annual values of SOC and AGB from 500 simulations (i.e., median of 95PPU bands). These simulations were carried out based on the 500 parameter set-samples generated from the optimized PUR under the multi-variable calibration approach (TableA2). We then used these 500 parameter set-samples to obtain annual values of SOC and AGB (i.e., median of 95PPU bands from 500 simulations) under a 10% lower grazing intensity regime by lowering fraction of plant biomass removed (*flgrem* parameter) by 10% in all parameter sample-sets, while keeping all other parameters constant. For each spatial unit, we obtained median values for SOC and AGB from the associated 95PPU bands of 500 simulations (i.e., output from the SUFI-2 algorithm) at a yearly time step, which were then averaged (i.e., M95PPU) over the two periods. We then compared the M95PPU values obtained for the two time periods to calculate the change in SOC and AGB under a given grazing intensity regimes. We used area-weighted average changes in SOC and AGB at the township scale to illustrate impacts of recent climate change on SOC and AGB under different grazing regimes across Alberta's native grasslands.

3. Results

3.1. Model parameter estimation

Most of the initially identified input parameters were sensitive to both SOC and AGB. The global sensitivity analysis indicated that 56 out of 88 parameters were sensitive to SOC and AGB (Table A1, Table A2). These were parameters related primarily to soil water (e.g., *fwloss(4)*) and nutrient dynamics (e.g., *riint*), litter and soil organic matter decomposition (e.g., *dec1(1)*), plant growth and production (e.g., *ppdf(1)*) as well as two parameters controlling grazing impacts (*flgrem*, *gret(1)*). The remaining 32 parameters were found to be much less sensitive to SOC and AGB (Table A1).

The initially suggested values for most of the input parameters were adjusted through different calibration approaches (Table A2). Across different grassland regions, the initial values for 22 parameters fell

outside their optimized PUR obtained based on single-variable calibration approaches. This pattern was observed for 31 parameters in the multi-variable calibration approach. 14 of these parameters control soil nutrient availability (e.g., *damr(1,1)*, *favail(1)*, *varat11(1,1)*, *snfxmx(1)*); nine parameters control litter and organic matter decomposition rate (e.g., *aneref(3)*, *dec4*, *peftxa*, *teff(1)*); five parameters control plant growth and production (e.g., *basetemp(1)*, *ppdf(1)*, *prdx(1)4_5*); two parameters control lignin content of plant materials (*fligni(1,1)*, *fligni(1,2)*); and one parameter (*fwloss(1)*) controls soil water content (Table A2, Table A1, Table A2).

The optimized PUR for most of the input parameters varied among calibration approaches (Table A2). Overall, the multi-variable calibration approach produced the narrowest PUR (on average narrowed 84% of initial ranges, varied from 56% to 94%), followed by the single-variable calibration approach of AGB (on average narrowed 80% of initial range, varied from 30% to 93%) and SOC (on average narrowed 76% of initial range, varied from 33% to 97%). Although the multi-variable calibration approach reduced the overall uncertainty as compared to the other two calibration approaches, the PUR varied among grassland regions. There were ten parameters under the multi-variable calibration approach with a wider PUR across regions as compared to the other parameters. Six of these parameters control plant growth and production (*basetemp(1)*, *ppdf(1)*, *ppdf(2)*, *ppdf(3)*, *ppdf(4)*, *rdrj*); two parameters control litter and organic matter decomposition rate (*dec2(2)*, *teff(2)*); one parameter (*riint*) controls soil nutrient availability; and one parameter (*fwloss(4)*) controls soil water content (Table A1, Table A2).

3.2. Model performance evaluation

The initial simulation was not able to accurately represent the spatiotemporal patterns of SOC and AGB measurements in different grassland regions (Fig. 3). Simulated SOC was smaller and AGB was greater in this initial simulation compared to the SOC and AGB measurements in all regions. Also, the initial simulation resulted in a relatively small correlation between the spatiotemporal patterns of simulated AGB and the corresponding remotely sensed AGB proxies (average correlation coefficient of 0.18, ranged from 0.10 to 0.25 across regions; Fig. 4).

The regionalized grassland carbon models accounted for the variability in the SOC and AGB measurements. However, model performance varied among calibration approaches and grassland regions (Fig. 3, Table 2). Across different regions, the single-variable calibration approach produced satisfactory simulation results, but only for the calibrated output variable (on average 66% and 56% of the SOC and AGB measurements fell within the 95PPU band, respectively). Besides, this approach resulted in a relatively greater correlation between simulated AGB and remotely sensed AGB proxies as compared to the initial simulation (Fig. 4). However, a greater correlation was found in the single-variable calibration approach of AGB (average coefficient of 0.44, ranged from 0.31 to 0.55 across regions) than in the SOC approach (average coefficient of 0.25, ranged from 0.18 to 0.33 across regions; Fig. 4).

In contrast to the single-variable approach, the multi-variable approach provided more reliable simulation results for both SOC and AGB (Fig. 3, Table 2). It accounted for more of the spatiotemporal variability in the SOC and AGB measurements across different regions (on average 67% of the total SOC and AGB measurements fell within the 95PPU band). In addition, the multi-variable approach (average *R-factor* of 1.36) compared to the single-variable approach of SOC and AGB (average *R-factor* of 1.47 and 1.71, respectively) resulted in reduced model simulation uncertainty across regions (Fig. 3, Table 2). Finally, the multi-variable approach yielded a considerably greater correlation between simulated AGB and remotely sensed AGB proxies (average coefficient of 0.61, ranged from 0.51 to 0.70 across regions) as compared to the single-variable approach. This pattern was persistent across different regions (Fig. 4).

3.3. Spatial distribution of SOC and AGB

The simulation results obtained based on the multi-variable calibration approach showed a pronounced variation in the spatial distribution of SOC (on average 48.6 ton/ha, ranged from 26.5 to 81.2 ton/ha) and AGB (on average 1326 kg/ha, ranged from 1031 to 2205 kg/ha) across different grassland regions (Fig. 5). As expected, a greater SOC (on average 80.2 ton/ha) and AGB (on average 1916 kg/ha) were estimated for the majority of spatial units in the Black soils of the Foothills and Parklands. However, the majority of spatial units in the Gray soils of the boreal Mixedwoods and the Brown soils of the prairies were characterized with a relatively smaller SOC (on average 60.5 and 32.9 ton/ha, respectively) and AGB (on average 1654 and 1148 kg/ha, respectively). The results of uncertainty analysis also showed a pronounced variation in the spatial distribution of uncertainty in the simulation of SOC and AGB across the regions. A smaller uncertainty in the simulation of SOC and AGB (smaller than 20 and 15%, respectively) was obtained for the majority of spatial units in the Black soils of the Foothills and Parklands and the Brown soils of the prairies. Whereas, the majority of spatial units in the Gray soils of the boreal Mixedwoods were characterized with relatively greater uncertainty in the simulation of SOC and AGB (>20 and 15%, respectively). Nevertheless, the spatial quantification of simulation uncertainty revealed a greater uncertainty in the simulation of SOC (on average 18.1%, ranged from 15.1% to 20.6%) than in the simulation of AGB (on average 14.5%, ranging from 11.5% to 18.2%) across grassland regions (Fig. 5).

3.4. Effects of recent climate change and grazing regimes on SOC and AGB

The spatial quantification of recent climatic changes between the 1970s and 2000s showed diverse patterns of changes in annual precipitation and minimum and maximum temperature across Alberta's grasslands (Fig. 6, Fig. 7). Overall, there was little observed change in annual precipitation between the 1970s and the 2000s. The annual precipitation increased slightly in the Brown soils of the prairies and the Black soils of the Foothills (except the southern part of the Foothills Fescue region). While, it decreased slightly in Gray soils of the Parklands and boreal Mixedwoods (Fig. 6, Fig. 7). In contrast to the annual precipitation, there was an overall increase in minimum and maximum temperature. The magnitude of this increase in annual temperature was greater for minimum temperature than for maximum temperature. However, this pattern of change in annual temperature varied across Alberta's grasslands. Specifically, the increase in minimum and maximum temperature was most apparent in the Gray soils of the Parklands and boreal Mixedwoods in central and northern Alberta (Fig. 6, Fig. 7).

The response of SOC and AGB to the recent changes in climate varied spatially across Alberta's grasslands (Fig. 8, Fig. 9). Under baseline grazing intensity regime, there was an overall decrease in the SOC between the 1970s and the 2000s. However, the magnitude of this decrease in the SOC was greater in the Black soils of the Foothills and Parklands and the Gray soils of the boreal Mixedwoods, while it was least apparent in the Brown soils of the prairies (Fig. 8, Fig. 9). In contrast to the SOC, the pattern of change in AGB in response to recent climate change was less consistent across Alberta's grasslands (Fig. 8, Fig. 9). Under baseline grazing intensity regime, the AGB decreased between two time periods in the Black soils of the Foothills and Parklands and the Gray soils of the Parklands and boreal Mixedwoods located in the central Alberta. While, it increased in the Brown soils of the prairies in the south and the majority of spatial units in the Gray soils of the boreal Mixedwoods located in the northern Alberta (Fig. 8, Fig. 9).

Under the proposed 10% lower grazing intensity regime, there was an overall increase or slight decrease in the SOC between the 1970s and the 2000s. The magnitude of increase in the SOC was greater in the Gray soils of the boreal Mixedwoods in the north, while a greater magnitude of the decrease in the SOC was observed

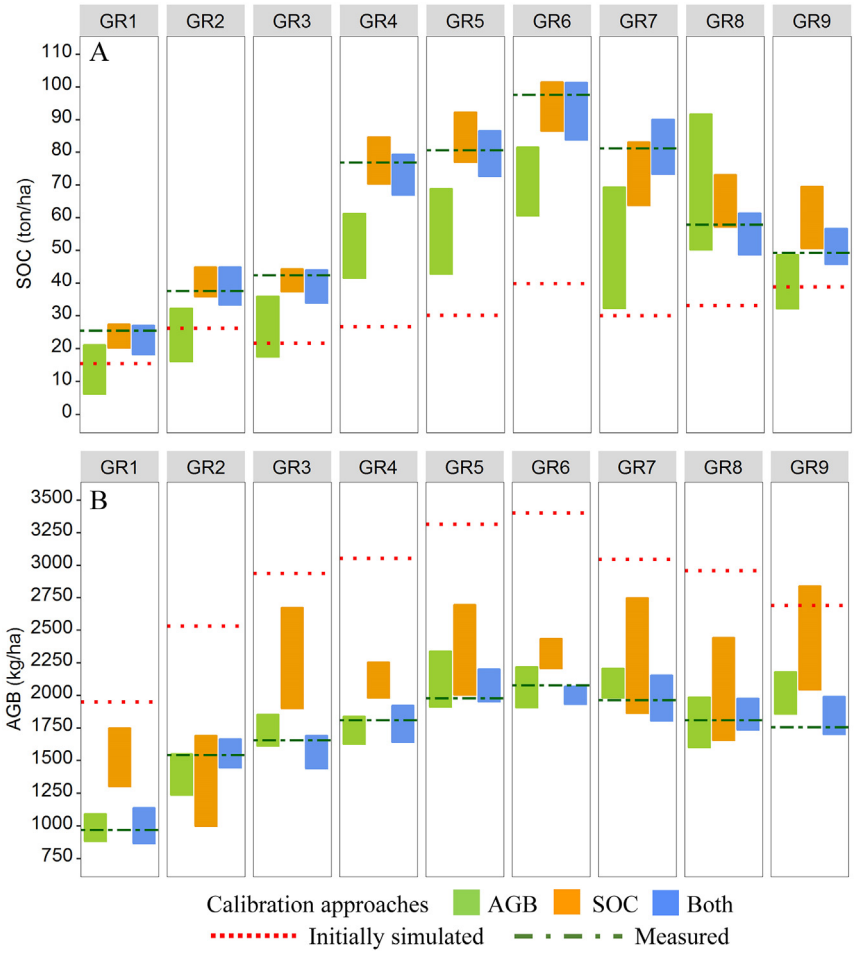

Fig. 3. Comparison of measured and simulated average SOC (A) and AGB (B) in spatial units with measured SOC and AGB in different grassland regions (GR). Simulated SOC and AGB are expressed as 95PPU bands based on the single- (SOC or AGB), and multi-variable (Both) calibration approaches.

in the Black soils of the Foothills and Parklands in the central Alberta (Fig. 8, Fig. 9). In contrast to the SOC, the pattern of recent change in AGB under the proposed lower grazing intensity regime was more consistent across Alberta's grasslands. Under the proposed 10% lower grazing intensity regime, there was an overall increase in the AGB between the 1970s and the 2000s, except for the Black and Gray soils of the Parklands in the central Alberta where the AGB decreased between two periods (Fig. 8, Fig. 9).

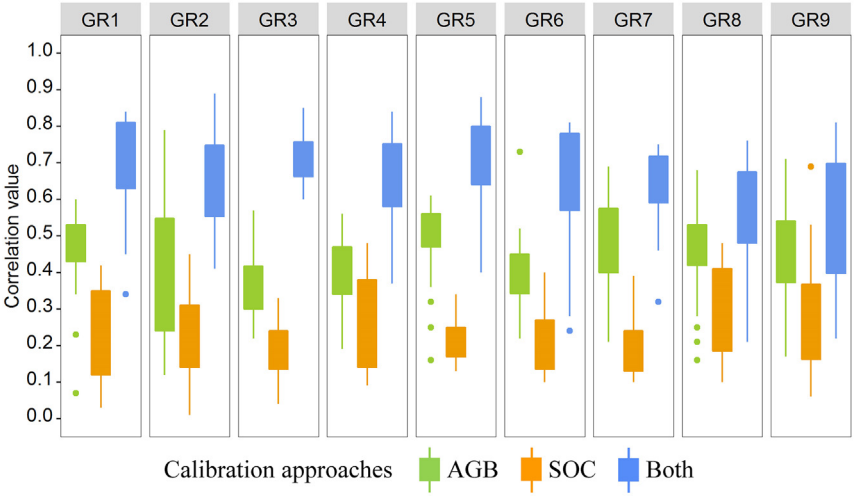

Fig. 4. Correlation between time series (2000−2010) of simulated AGB and the corresponding remotely sensed AGB proxies in different grassland regions. Boxplots show variation in the average regional correlation values obtained from the simulation results of the single- (SOC or AGB) and multi-variable (Both) calibration approaches (500 average values per approach per region).

Table 2
Calibration performance of the regionalized grassland carbon models developed using the single- (SOC or AGB), and multi-variable (Both) calibration approaches.

Region	Calibration variable	No. sites	No. measurements	Objective function		Calibration & uncertainty index	
				PBIAS	*RSR*	*P-factor*	*R-factor*
GR1	SOC	66	264	24.3	1.23	0.67	0.79
	AGB	18	302	18.7	1.32	0.57	1.54
	Both	84	566	11.7	1.10	0.72	1.27
GR2	SOC	29	116	15.7	1.03	0.69	1.07
	AGB	10	205	21.0	1.30	0.59	1.97
	Both	39	321	21.9	1.09	0.69	1.18
GR3	SOC	41	164	10.7	0.85	0.68	0.79
	AGB	11	203	23.5	1.13	0.57	1.44
	Both	52	367	17.7	0.93	0.70	1.14
GR4	SOC	32	128	23.7	1.16	0.63	1.52
	AGB	10	181	12.9	1.03	0.56	1.35
	Both	42	309	17.4	1.01	0.65	1.50
GR5	SOC	25	100	14.5	0.87	0.65	1.62
	AGB	8	192	25.3	1.15	0.59	2.41
	Both	33	292	12.0	1.06	0.68	1.34
GR6	SOC	26	104	28.4	0.92	0.66	1.60
	AGB	9	157	11.8	1.17	0.53	1.81
	Both	35	261	14.2	0.93	0.67	1.29
GR7	SOC	43	172	19.7	0.90	0.69	2.07
	AGB	10	211	17.0	0.85	0.55	1.35
	Both	53	383	19.9	0.93	0.67	1.78
GR8	SOC	40	160	26.1	1.15	0.61	1.67
	AGB	9	156	21.4	1.35	0.56	2.17
	Both	49	316	23.3	1.00	0.60	1.54
GR9	SOC	28	112	23.5	0.99	0.64	2.05
	AGB	8	176	26.1	1.29	0.52	1.32
	Both	36	288	18.5	1.13	0.60	1.47
All regions	SOC	330	1320	20.7	1.01	0.66	1.47
	AGB	93	1783	19.7	1.18	0.56	1.71
	Both	423	3103	17.4	1.02	0.67	1.39

4. Discussion

4.1. Model parameter estimation and performance evaluation

4.1.1. Sensitive model parameters

Overall, most of the initially identified parameters were sensitive to both SOC and AGB. However, 32 parameters that we found to be less sensitive to SOC and AGB (Table A1) have been reported in the literature to be important controllers of SOC dynamics. The results of sensitivity analysis vary depending on whether multiple (i.e., both SOC and AGB) or single model outputs (i.e., SOC or AGB only) are considered (Rafique et al., 2013; Faramarzi et al., 2017). Also, the results of sensitivity analysis conducted for a specific geographic area may not be directly applicable to other areas (Gilmanov et al., 1997; Abbaspour et al., 2007; Wang et al., 2013; Faramarzi et al., 2015; Necpálová et al., 2015; Dimassi et al., 2018). Nevertheless, different results for sensitive and less sensitive parameters could be obtained if more accurate historic climate and land use information (i.e., grazing management) were used in the initial model set up. Also, we are not sure if the results of our sensitivity analysis would have been different if we had conducted a sensitivity analysis for each grassland region, separately.

4.1.2. Performance of initial model

Our initial simulation was not able to accurately represent the spatiotemporal patterns of SOC and AGB across different grassland regions. Inaccurate estimates obtained from the initial simulation points to shortcomings in prior knowledge and expert opinion as inputs to the simulation of carbon-related ES in grasslands, particularly under new ecological conditions (Smith et al., 1997a; Rafique et al., 2015; Kwon et al., 2017; Dimassi et al., 2018). Our regionalized parameterization and calibration scheme resulted in adjusted values for most of the sensitive input parameters under different calibration approaches. Therefore, initial parameter values suggested in the previous modeling studies must be cautiously employed as they may not necessarily represent ecological and land use characteristics of other geographic regions (Smith et al., 1997a; Rafique et al., 2015; Dimassi et al., 2018). Algorithmic parameter estimation enables a deeper understanding of the behavior of model parameters and functions through extracting maximum information from measured data collected under local conditions (Necpálová et al., 2015).

4.1.3. Model performance under single-variable calibration approach

Compared to the initial simulation, the regionalized carbon models developed under the single-variable calibration approach of SOC and AGB produced satisfactory simulation results across different regions, but conditional on the type of output variable considered in calibration and validation process. These findings suggest that partial calibration of an ecosystem carbon model (i.e., against SOC or AGB measurements alone) cannot provide reliable estimates for other carbon-related ES across diverse grasslands with a wide range of variation in climate, soil, vegetation, and land management conditions. In the algorithmic calibration of complex ecosystem models, a large number of input parameters are allowed to vary within a wide PUR to achieve the best fit between simulated and measured values (Abbaspour et al., 2007; Niquil et al., 2011; Rafique et al., 2015). However, there is a risk of over calibration with this approach where a wrong model structure with unrealistic model parameters but with acceptable calibration performance can be achieved (Faramarzi et al., 2015). Precisely, this may happen in the partial calibration of ecosystem models, when there is a strong correlation among parameters, so that changes in one parameter can be compensated by changes in other parameters (Meersmans et al., 2013; Kwon et al., 2017). Hence, the performance of such partially calibrated model, as indicated by the single-variable approach of SOC or AGB in the present study, is conditional on the type of output variable considered in calibration and validation process (Gupta et al., 1998; Faramarzi et al., 2017). In other words, the partially calibrated model might not necessarily result in a reliable simulation of output variables representing other interrelated biophysical processes (Niquil et al., 2011; Rafique et al., 2013).

Nevertheless, in the present study, calibration based on the SOC measurements (i.e., SOC approach) produced relatively better simulation results of AGB in the most productive Black soils of the Foothills and Parklands. Whereas, calibration based on the AGB measurements (i.e., AGB approach) resulted in relatively better simulation results of SOC in the least productive Brown soils of the prairies (Table 1, Table 2). This pattern suggests that in the higher productive grasslands, the dynamics of organic carbon and its fraction in soil or plant biomass might be regulated by belowground processes (i.e., decomposition rate and nutrient availability). However, it might be controlled by aboveground processes (i.e., plant growth and productivity, biomass removal) in the lower productive grasslands (Schimel et al., 1994; Cerri et al., 2007; Adhikari and Hartemink, 2016; Hewins et al., 2018; Wiesmeier et al., 2019). Further field studies are needed to prove or disprove this hypothesis. Results from such studies may lead to a more reliable and efficient field monitoring and assessment of the carbon-related ES in grasslands distributed over vast geographic areas.

4.1.4. Model performance under multi-variable calibration approach

In contrast to the single-variable approach, the regionalized carbon models developed under the multi-variable calibration approach produced satisfactory simulation results and reduced simulation uncertainty for both SOC and AGB across regions. Incorporating additional variables into calibration scheme has been recommended as one of the effective approaches to cope with over calibration issue in the algorithmic calibration of complex biogeochemical ecosystem models (Gupta et al., 1998; Abbaspour et al., 2007; Faramarzi et al., 2015). The provision of carbon-related ES in grasslands is closely associated with the historical balance between the rate of plant productivity and the

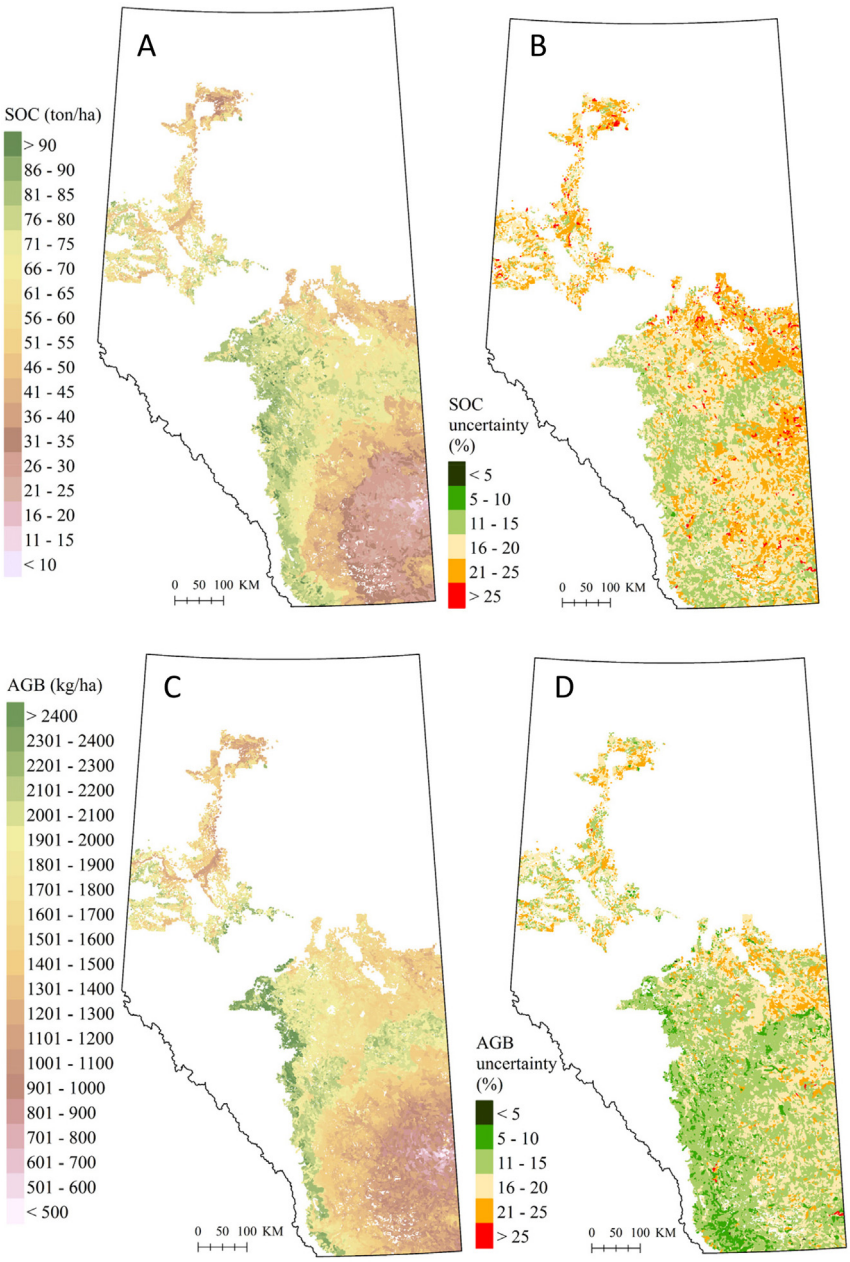

Fig. 5. Simulated average (2000–2010) SOC (A) and AGB (C) and their associated uncertainties (B, and D, respectively) across Alberta's native grasslands. The boundaries of native grassland areas are thickened for better visualization (see Fig. 1 for the exact areas of grasslands).

rate of decomposition of the organic compounds and residues stored in the soil (Blair et al., 2014; Adhikari and Hartemink, 2016; Hungate et al., 2017). In our multi-variable calibration approach, we targeted these two key interrelated biophysical processes by integrating field measurements data on AGB and SOC into a multi-stage calibration scheme, where at each stage a specific process was calibrated. In addition, the provision of carbon-related ES is highly variable in both time (i.e., much faster rate of change in AGB than in SOC) and space (i.e., under varying ecological conditions) over a large geographic area (Parton et al., 1987; Schimel et al., 1994; Van den Bygaart et al., 2008; Oelbermann and Voroney, 2011; Xiong et al., 2015; Wiesmeier et al., 2019). The SOC and AGB measurements employed in this study were at different spatial and temporal resolution; the SOC data were single-time measurements collected from a greater number of grassland sites, while the AGB data were long-term time series measurements obtained from a smaller number of sites, compared to the SOC measurements. Thus, integrating both types of spatially and temporally different field measurements into a calibration scheme improved model performance and reduced simulation uncertainty by proper simulation of the spatiotemporal dynamics of the relevant biophysical processes.

Our simulation results showed that on average 67% of spatial and temporal variability in both SOC and AGB measurements were captured across regions (Table 2). This imperfection may, to some extent, demonstrate the lack of high quality measured data, and limitation in model structure and conceptual assumptions such as below-ground plant productivity and nutrient availability (Schimel et al., 1994; Cerri et al., 2007; Adhikari and Hartemink, 2016; Hewins et al., 2018; Wiesmeier et al., 2019) that we did not include in our regionalized calibration scheme. Determining key biophysical processes controlling the provision of carbon-related ES across geographically wide grassland areas can lead to a more robust calibration of biogeochemical ecosystem model, thus a more reliable estimates of carbon-related ES.

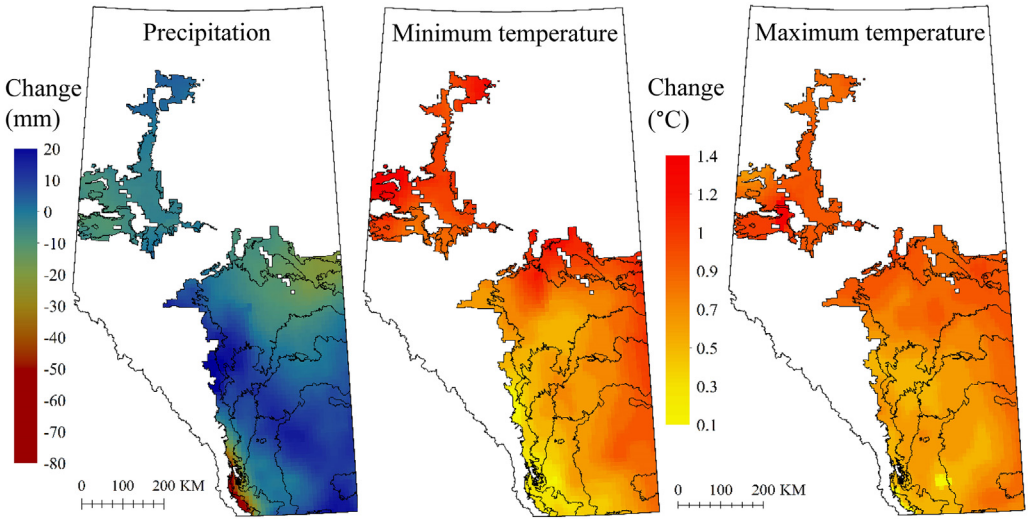

Fig. 6. Spatial patterns of change in annual precipitation (left) and minimum (middle) and maximum temperature (right) between the 1970s (1961–1980) and the 2000s (1991–2010). Values are area-weighted average changes in precipitation and temperature at the township scale. Dark lines represent the boundary of different grassland regions.

The multi-variable approach narrowed the initial PUR the most (Table A2). The algorithmic parameter estimation has been applied to DayCent ecosystem model (i.e., the daily time-step version of the CENTURY model) at a much smaller spatial extent, but only optimized parameter values instead of optimized PUR were reported (e.g., Rafique et al., 2013). However, the algorithmic parameter estimation with measurements from multiple ES has been employed by researchers in other scientific disciplines to narrow the defined PUR the most (Gupta et al., 1998 and its citations), thus helping to reduce the non-uniqueness problem while reducing uncertainty prediction (Abbaspour et al., 2007).

The optimized PUR obtained through the multi-variable calibration approach varied among grassland regions. Varying ecological conditions across the province can explain the variation in optimized PUR across different regions. Alberta's grasslands are characterized by distinct ecological regions with diverse vegetation (Fig. 1, Table 1; Downing and Pettapiece, 2006), resulting in high spatial variability in the production of carbon-related ES (Ogle et al., 2007; Hewins et al., 2018). Climatic (e.g., precipitation, temperature), edaphic (e.g., soil texture, structure, nutrient availability) and biotic factors (e.g., plant and microbial diversity, grazing) predominantly control the provision of carbon-related ES in grasslands (Parton et al., 1987; Schimel et al., 1994; Álvaro-Fuentes et al., 2012; Abdalla et al., 2018; Wiesmeier et al., 2019). In the CENTURY model, plant growth and production and soil carbon dynamics are closely linked through the nutrient and water cycles (Parton et al., 1988). Besides, the lignin content of plant materials has significant control over litter and organic matter decomposition rate (Murphy et al., 2002). Consequently, the processes involved in the provision of carbon-related ES can be substantially altered by ecological conditions of the grassland systems (Hou et al., 2013; Xiong et al., 2015; Hewins et al., 2018). Spatial variation in our optimized PUR represented such ecological variability, resulting in a more reliable and representative model than simplified models in earlier studies. The CENTURY model has been previously used to assess the dynamics of SOC across a series of grassland sites with varying climatic conditions, where the interaction of sensitive processes and their spatial variability were not fully considered (e.g., Schimel et al., 1994; Smith et al., 1997a; Lugato et al., 2014). To the best of our knowledge, this is the first time this model has been calibrated by accounting for interaction among model parameters to achieve optimized PUR for a range of distinct grassland systems over a large geographic area.

4.2. Uncertainty in SOC and AGB simulation

As expected, our simulation results revealed a pronounced variation in the spatial distribution of SOC and AGB across different regions. However, the level of uncertainty in the simulation of SOC and AGB also varied across regions. The variation in simulation uncertainty across grassland regions can be explained by quantity and quality of field measurements used in our regionalized calibration scheme (Abbaspour et al., 2007; Rafique et al., 2013; Faramarzi et al., 2015; Sándor et al., 2018). The spatial heterogeneity represented by SOC and AGB

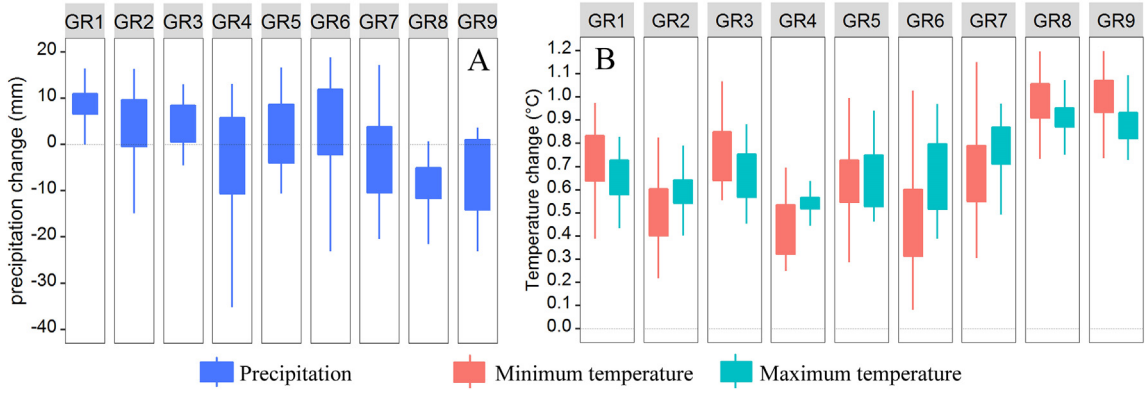

Fig. 7. Change in annual precipitation (A) and minimum and maximum temperature (B) between the 1970s (1961–1980) and the 2000s (1991–2010). Box plots show variation in recent climatic changes at the regional scale.

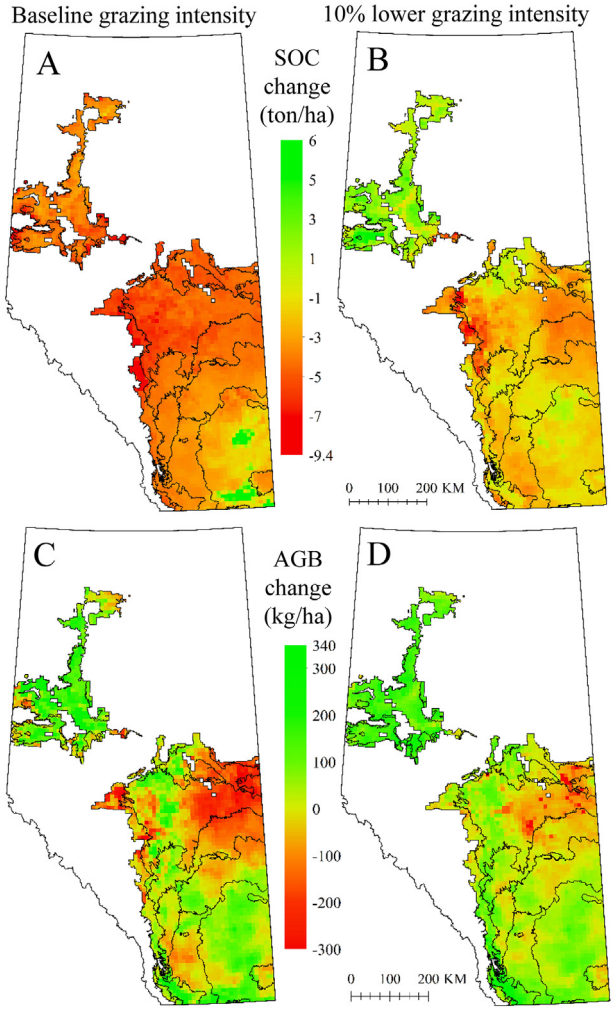

Fig. 8. Spatial patterns of the simulated change in SOC (top: A, B) and AGB (bottom: C, D) between the 1970s (1961–1980) and 2000s (1991–2010) under baseline grazing intensity (left: A, C) and a proposed 10% lower grazing intensity regime (right: B, D). Values are area-weighted average changes of 500 simulations at the township scale. Dark lines represent the boundary of different grassland regions.

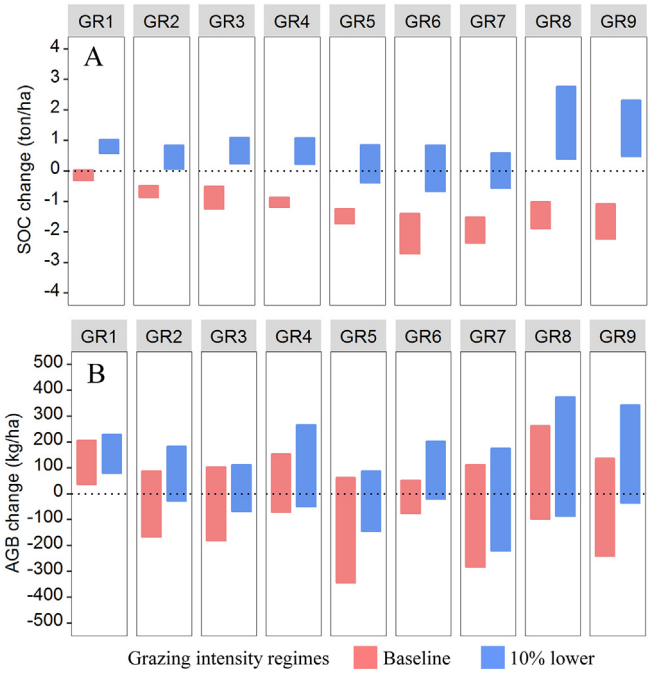

Fig. 9. Uncertainty in the response of SOC (A) and AGB (B) to the recent climate change under different grazing intensity regimes. Boxes show variation in the area-weighted average changes of 500 simulations at regional scale.

measurements differed among the regions, which significantly affected our model performance. The poorest model performance that obtained in the Gray soils of the boreal Mixedwoods in all regions (on average 61% of the total measurements fell within the 95PPU band) was related to the areas where the smallest proportion of spatial heterogeneity was represented by SOC and AGB measurements (Table 1, Table 2). As a result, these regions were characterized by relatively greater uncertainty in the simulation of SOC and AGB (Table 2, Fig. 5). In contrast, in the Brown soils of the prairies and in the Black soils of the Foothills and Parklands, where a greater proportion of spatial heterogeneity was represented by measured data (Table 1, Table 2), a relatively better model performance (on average 70 and 67% of the total measurements fell within the 95PPU band, respectively) and a smaller uncertainty in the simulation of SOC and AGB was obtained (Table 2, Fig. 5). These findings collectively demonstrate the importance of field measurements for SOC and AGB simulations in regional scale modeling. This calls for a systematic monitoring strategy, e.g., based on appropriate land stratification (i.e., stratified spatial heterogeneity) and sample size allocation to strata (i.e., efficient sampling design), which is crucial for reliable estimation of model parameters and supply of carbon-related ES across a wide range of grassland systems (Hou et al., 2013; Campbell and Paustian, 2015; de Gruijter et al., 2016).

Our spatial quantification of the simulation uncertainty revealed a greater uncertainty in the simulation of SOC than in the simulation of AGB across various regions. It is noteworthy that we initially expected a smaller uncertainty in the simulation of SOC than in the simulation of AGB due to a relatively higher spatial resolution and a greater number of SOC measurements within each region. However, the possible trade-off between the spatial and temporal resolution of two measurement types and their effects in calibration and simulation procedure resulted in a smaller uncertainty in the simulation of AGB than that of SOC. In our multi-variable calibration approach, the lower spatial resolution of AGB measurement may be compensated by the higher spatial resolution of SOC measurements. However, the higher temporal resolution of AGB measurements may not offset the lack of temporal resolution in SOC measurements to the same extent. Moreover, ambiguity created by extrapolating SOC measurements to the first 20 cm depth of grassland soil may contribute to the resulted error in the simulation of SOC. Therefore, both spatial and temporal resolution at which the field measurements are collected play a pivotal role in reliable simulation of carbon-related ES across a wide geographic area with heterogeneous ecological conditions (Cleveland et al., 1999; Ogle et al., 2010; Xiong et al., 2015; Sándor et al., 2018; Wiesmeier et al., 2019). In the past few decades, the remotely sensed data has been widely integrated with the sparsely ground-based measurements to obtain high spatiotemporal information on ecosystem functioning and services (Cord et al., 2017). In this study, we integrated remotely sensed AGB proxies for the 2000 to 2010 period in the model validation. Further research studies are needed for the full integration and assessment of remotely sensed information on soil properties and vegetation growth and quality (i.e., lignin content of plant materials) to improve the spatially-explicit simulation of carbon-related ES across a wide range of grassland systems.

4.3. Response of SOC and AGB to recent climate change and grazing regimes

Our simulation results under baseline condition (i.e., using the optimized PUR for sensitive parameters) revealed an overall negative effect of recent climatic changes on the SOC, while a less consistent effect on the AGB across Alberta's native grasslands. As expected, the magnitude

of the decrease in the SOC was greater in the Gray soils of the boreal Mixedwoods in the central and northern Alberta, where recent climatic changes resulted in a slight dryer but a considerably warmer climate. In contrast to the SOC, our simulation results of the AGB in this area showed a wide range of uncertainty in effect of recent climate change, ranging from a negative effect to a considerably positive impact on the AGB. The poor regional model performance obtained in the Gray soils of the boreal Mixedwoods might explain this unexpected pattern of effect on the AGB. However, our simulation results also revealed an unexpected pattern of effect in high productive Black soils of the Foothills and Parklands in central Alberta, where a satisfactory model performance was obtained. Our assessment of recent climate change in this latter area showed only a slight increase in both annual precipitation and temperature, but our simulation results overall showed a noticeable negative impact of recent climatic changes on both SOC and AGB. These findings collectively suggest that the responses of carbon-related ES to stressors such as climate change may vary in direction and magnitude depending on the ecological conditions of grasslands (Lopez-Marsico et al., 2015; Abdalla et al., 2018). The observed heterogeneity in the magnitude and direction of the climate change impacts on the SOC and AGB indicates that the likely climate change risks and opportunities for carbon-related ES differ spatially across Alberta's grasslands. Previous studies have also showed a wide-ranging effects of climate change on different carbon-related ES (Li et al., 2018) mainly related to the direction and magnitude of change in precipitation and temperature patterns, and environmental conditions of sites studied (e.g., Parton et al., 1995; Smith et al., 2009; Álvaro-Fuentes et al., 2012; Abdalla et al., 2018)

Land management choices such as changes in grazing intensity regime have been suggested as the primary means of adapting to climate change-driven alterations in carbon-related ES (Havstad et al., 2007; Daily et al., 2009; Li et al., 2018; Jellinek et al., 2019). A comprehensive assessment of the impacts of recent climate change on the provision of carbon-related ES under alternative grazing practices can help better understand the effectiveness of such potential climate change adaptation strategies. To examine if grazing management can serve as a potential adaptation strategy to maintain carbon-related ES in Alberta's grasslands, we assessed the response of SOC and AGB to recent climatic changes under baseline grazing intensity regime (i.e., using the PUR obtained for the sensitive grazing parameters) and a proposed 10% lower grazing intensity regime. In contrast to the baseline grazing intensity regime, our simulation results under the 10% lower grazing regime revealed an overall positive or slightly negative impact of recent climate change on the SOC and an overall positive impact on the AGB across Alberta's grasslands. However, the magnitude of the positive impact on both SOC and AGB was greater in the Gray soils of the boreal Mixedwoods in the north and in less productive Brown Soils of the prairies in the south, where different patterns of recent climatic changes were observed. Also, in the high productive Black soils of the Foothills and Parklands, the 10% lower grazing intensity regime compared to the baseline grazing intensity regime decreased the negative impacts of recent climate change on both SOC and AGB, but only in the area where a slight change in annual precipitation and temperature was observed. These findings collectively demonstrate that grazing management has the potential to be a beneficial adaptation strategy to properly manage the impacts of climate change on the provision of carbon-related ES. However, the spatial variability in the magnitude and effectiveness of the proposed 10% lower grazing intensity as a potential adaptation strategy to maintain the SOC and AGB indicates that best grazing practices to maintain the provision of carbon-related ES under a changing climate will be region-specific. Inconsistent effect of grazing intensity management on the SOC and AGB has been reported from the grassland systems characterized by different grazing history and ecological and environmental conditions (e.g., Abdalla et al., 2018).

The biogeochemical ecosystem models have been applied in a few studies to assess the impacts of grazing management on carbon-related ES across wide geographic areas (e.g., Wang et al., 2008; Feng and Zhao, 2011; Chang et al., 2015; Lopez-Marsico et al., 2015). However, the uncertainty related to the spatial variation in grazing intensity was rarely considered. The CENTURY model deals with the impacts of grazing on the system through herbage removal and the return of nutrients by animals, both altering the C: N ratio in the soil and plant materials (Parton et al., 1988). Calibration results of the multi-variable approach showed a wide PUR for the fraction of shoots removed by grazing (*flgrem* parameter) across regions (30–69%), representing variation in grazing intensity by land tenure and other environmental and management factors across the landscape (Van den Bygaart et al., 2008; Blair et al., 2014; Wang et al., 2014; Chang et al., 2015). It is usually challenging to measure parameters describing grazing impacts directly and such field data are generally lacking for large-scale modeling (Feng and Zhao, 2011). Therefore, the algorithmic approach used in the present study to quantify spatial uncertainty in grazing intensity can be employed as a practical approach to deal with uncertainty related to lack of grazing data in the spatially explicit assessment of carbon-related ES and their associated uncertainty over a large geographic area.

The proposed 10% lower grazing intensity regime represents one example of how our regionalized parameterization and calibration scheme can be employed to increase the level of confidence in using the simulation results to inform grazing management decisions in grassland systems distributed over vast geographic areas. Lowering grazing intensity by decreasing the cattle stocking rate may reduce a rancher's income (i.e., via the sale of beef cattle). Therefore, determining how a rancher's total income would change in response to altering cattle stocking rate help understand better if implementing a lower grazing intensity regime is an appropriate adaptation to maintain carbon-related ES in Alberta's grasslands under a changing climate (Havstad et al., 2007; Jack et al., 2008; Li et al., 2018; Jellinek et al., 2019).

5. Conclusion

Through a comprehensive parameterization and calibration of the ecosystem model CENTURY, we found that simulations based on prior knowledge and expert opinion alone, or based on partial calibration of an ecosystem carbon model may not lead to reliable estimates of carbon-related ES across a diverse range of grassland systems. Instead, robust simulation results are possible using a regionalized parameterization and calibration scheme based on a multi-variable calibration approach in which data and information representing key biophysical processes are integrated simultaneously into calibration analysis. Therefore, it is pivotal to obtain spatial and temporal field measurements through appropriate and efficient sampling design. High spatial and temporal resolution data produced through the integration of sparse ground-based measurements with remotely sensed information on key ecosystem functions and services could lead us to improved model structure and a more reliable estimation of carbon-related ES across a diverse range of ecological conditions.

Our assessment of the response of SOC and AGB to recent climatic changes showed varied patterns of response across grassland regions, suggesting needs for a range of strategies for adaptation to the likely risks associated with climate change across Alberta's grasslands. In addition, our assessment of the response of SOC and AGB to recent climatic changes under a proposed 10% lower grazing intensity regime revealed that the effectiveness of grazing intensity management as a potential adaptation strategy to maintain and properly manage carbon-related ES will be region-specific.

This study provides a strong foundation for assessing the current status of SOC and AGB and associated uncertainties in grassland systems across western Canada and other geographically broad areas. The modeling framework developed in this study provides the basis for further assessment of the potential effects of future climate and land use change in identifying alternative adaptive management scenarios that

potentially ensure long-term provision of carbon-related ES in grassland systems. Other applicable and relevant grazing scenarios, including those that vary grazing season duration or region of application of different grazing intensity regimes, need to be considered for further assessments.

Acknowledgments

We gratefully acknowledge funding from the Alberta Innovates (Grant # BIO-12-006), the Alberta Agriculture and Forestry (Grants # 2012S007S & 2016E017R), the Natural Sciences and Engineering Research Council of Canada Discovery Grants Program (Grant # RES0043463), and the Campus Alberta Innovation Program (CAIP) Chair Award (Grant # RES0034497). We thank the Rangeland Branch of Alberta Environment and Parks for providing information on long-term trends in grassland biomass production across the province of Alberta. We appreciate constructive comments from anonymous referees. We also appreciate feedback from Carlos Tornquist, Todd Campbell, Amy Nixon, Carrie Selin, Craig DeMaere, Donna Lawrence, Cameron Carlyle, and Edward Bork on this work.

Appendix A

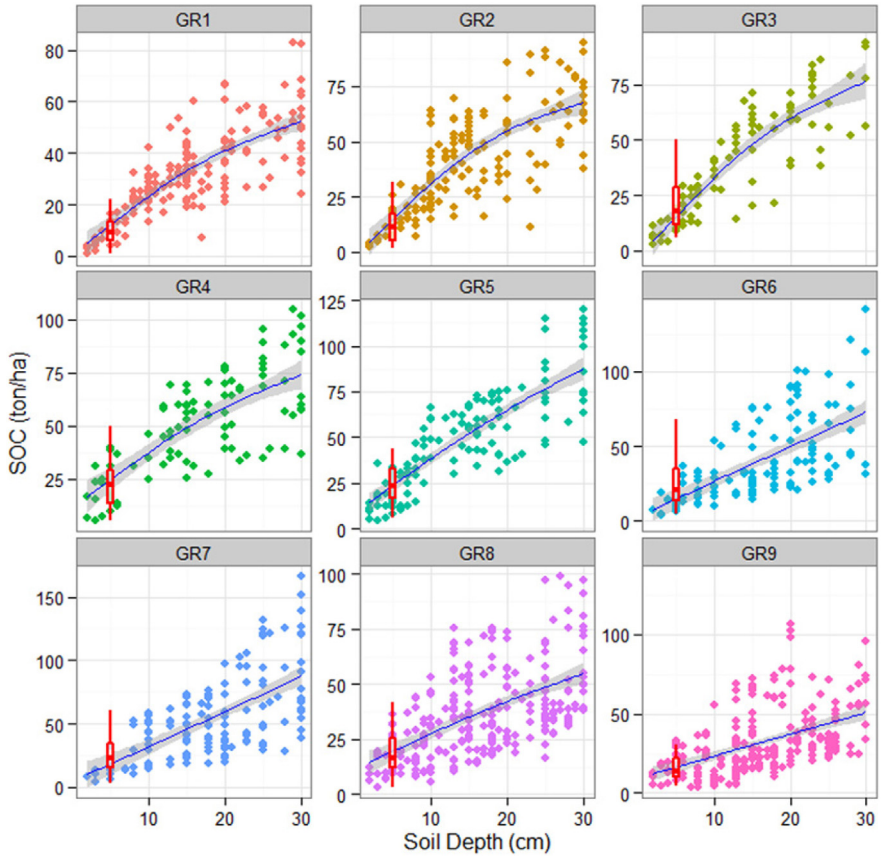

Fig. A1. The best-fit regression lines representing depth distribution of SOC in different grassland regions. The red boxes show variation in SOC measured in the top 5 cm depth of mineral soil at ABMI grassland monitoring sites associated with different regions. The regional conversion factors, derived from the established regression models (based on the fitted SOC values at 5 and 20 cm depth), were used to extrapolate ABMI's SOC measurements to the first 20 cm depth of grassland soil.

Table A1
The CENTURY input parameters considered for sensitivity analysis (underlined: most sensitive; not underlined: less sensitive) with their initial values (used in initial simulation) and parameter uncertainty ranges (PUR) defined for Alberta's grasslands.

Parameter	Type	Definition	Unit	Initial value	Defined PUR	
					Min	Max
aneref(1)	Fixed	Ratio of rain or potential evapotranspiration below which there is no negative impact of soil anaerobic conditions on decomposition	ratio	1.5	0.5	2
aneref(2)	Fixed	Ratio of rain or potential evapotranspiration above which there is maximum negative impact of soil anaerobic conditions on decomposition	ratio	3	2	4
aneref(3)	Fixed	Minimum value of the impact of soil anaerobic conditions on decomposition.	unitless	0.3	0.1	0.8
damr(1,1)	Fixed	Fraction of surface N absorbed by residue	fraction	0.03	0.001	0.2
damr(1,2)	Fixed	Fraction of surface P absorbed by residue	fraction	0.03	0.001	0.2
damr(2,1)	Fixed	Fraction of soil N absorbed by residue	fraction	0.02	0.001	0.2
damrmn(1)	Fixed	Minimum C/N ratio allowed in residue after direct absorption of N	ratio	15	5	20
dec1(1)	Fixed	Maximum surface structural decomposition rate, the fraction of the pool that turns over each year	g C month^{-1}	3.9	1	7

Table A1 (*continued*)

Parameter	Type	Definition	Unit	Initial value	Defined PUR	
					Min	Max
dec1(2)	Fixed	Maximum soil structural decomposition rate, the fraction of the pool that turns over each year	g C month^{-1}	4.9	2	8
dec2(1)	Fixed	Maximum surface metabolic decomposition rate, the fraction of the pool that turns over each year	g C month^{-1}	14.8	10	20
dec2(2)	Fixed	Maximum soil metabolic decomposition rate, the fraction of the pool that turns over each year	g C month^{-1}	18.5	13.5	23.5
dec3(1)	Fixed	Maximum decomposition rate of surface organic matter with active turnover, the fraction of the pool that turns over each year	g C month^{-1}	6	4	10
dec3(2)	Fixed	Maximum decomposition rate of soil organic matter with active turnover, the fraction of the pool that turns over each year	g C month^{-1}	7.3	4.3	10.3
dec4	Fixed	Maximum decomposition rate of soil organic matter with slow turnover, the fraction of the pool that turns over each year	g C month^{-1}	0.0045	0.001	0.03
dec5(1)	Fixed	Maximum decomposition rate of surface organic matter with intermediate turnover which is the fraction of the pool that turns over each year	g C month^{-1}	0.2	0.05	0.3
dec5(2)	Fixed	Maximum decomposition rate of soil organic matter with intermediate turnover rate	g C month^{-1}	0.2	0.05	0.3
deck5	Fixed	Available soil water content at which shoot and root death rates are half maximum	cm	5	3	7
elitst	Fixed	Effect of litter on soil temperature relative to live and standing dead biomass	unitless	0.4	0.25	0.55
favail(1)	Fixed	Fraction of N available per month to plants	fraction	0.9	0.1	0.95
favail(4)	Fixed	Minimum fraction of P available per month to plants	fraction	0.2	0.1	0.4
favail(5)	Fixed	Maximum fraction of P available per month to plants	fraction	0.4	0.3	0.8
favail(6)	Fixed	Mineral N in surface layer corresponding to maximum fraction of P available	g N m^{-2}	2	0.5	5
fleach(1)	Fixed	Intercept value used to compute the fraction of mineral N which will leach to the next layer when there is saturated water flow The flow depends on the sand content	fraction	0.2	0.1	0.8
fleach(2)	Fixed	Slope value to compute the fraction of mineral N which will leach to the next layer when there is a saturated water flow	fraction	0.7	0.1	0.8
fwloss(1)	Fixed	Scaling factor for interception and evaporation of precipitation by live and standing dead biomass	unitless	0.8	0.2	1.4
fwloss(2)	Fixed	Scaling factor for bare soil evaporation of precipitation (H2O loss)	unitless	0.8	0.2	1.4
fwloss(3)	Fixed	Scaling factor for transpiration water loss (H2O loss)	unitless	0.65	0.2	1.2
fwloss(4)	Fixed	Scaling factor for potential evapotranspiration	unitless	0.8	0.2	1.2
omlech(1)	Fixed	Intercept for the effect of sand on leaching of organic compounds	unitless	0.03	0.01	0.1
omlech(2)	Fixed	Slope for the effect of sand on leaching of organic compounds	unitless	0.12	0.03	0.12
pabres	Fixed	Amount of residue which will give maximum direct absorption of N	g C m^{-2}	100	70	130
pcemic (1,1)	Fixed	Maximum C/N ratio for surface microbial pool	ratio	20	15	25
pcemic (2,1)	Fixed	Minimum C/N ratio for surface microbial pool	ratio	10	5	15
peftxa	Fixed	Intercept parameter for regression equation to compute the effect of soil texture on the microbe decomposition rate	unitless	0.25	0.1	1
peftxb	Fixed	Slope parameter for the regression equation to compute the effect of soil texture on the microbe decomposition rate; the slope is multiplied by the sand content fraction	unitless	0.75	0.2	0.9
rcestr(1)	Fixed	C/N ratio for structural material	ratio	200	50	350
rcestr(2)	Fixed	C/P ratio for structural material	ratio	500	300	700
riint	Fixed	Root impact intercept used for calculating the impact of root biomass on nutrient availability	unitless	0.8	0.6	0.9
teff(1)	Fixed	"x" location of inflection point, for determining the temperature component of decomposition factor (DEFAC)	unitless	15.4	5	20
teff(2)	Fixed	"y" location of inflection point, for determining the temperature component of the DEFAC	unitless	11.75	5	15
teff(3)	Fixed	Step size (difference between the maximum point to the minimum point), for determining the temperature component of the DEFAC	unitless	29.7	20	40
teff(4)	Fixed	Slope of line at inflection point, for determining the temperature component of the DEFAC	unitless	0.031	0.01	0.07
varat11 (1,1)	Fixed	Maximum C/N ratio for material entering surface som1	ratio	14	8	30
varat11 (2,1)	Fixed	Minimum C/N ratio for material entering surface som1	ratio	3	1	7
varat12 (1,1)	Fixed	Maximum C/N ratio for material entering soil som1	ratio	14	10	20
varat12 (2,1)	Fixed	Minimum C/N ratio for material entering soil som1	ratio	3	1	9
basetemp (1)	Crop	Base temperature for plant growth	°C	7	3	10
basetemp (2)	Crop	Ceiling on the maximum temperature used to accumulate growing degree days	°C	30	25	40
biok5	Crop	Level of aboveground standing dead at which production is reduced to half maximum due to physical obstruction by dead material	g C m-2	60	20	100
biomax	Crop	Biomass level above which the minimum and maximum C/N or P ratios of new shoot increments equal pramn (*,2) and pramx(*,2) respectively	g biomass m-2	400	100	700
cfrtcn(1)	Crop	Maximum fraction of C allocated to roots under maximum nutrient stress	fraction	0.6	0.3	1
cfrtcn(2)	Crop	Minimum fraction of C allocated to roots with no nutrient stress	fraction	0.3	0.1	0.6
cfrtcw(1)	Crop	Maximum fraction of C allocated to roots under maximum water stress	fraction	0.6	0.3	1
cfrtcw(2)	Crop	Minimum fraction of C allocated to roots with no water stress	fraction	0.3	0.1	0.6
crprtf(1)	Crop	Fraction of N retranslocated from grass leaves at death	fraction	0.3	0.05	0.75
crprtf(2)	Crop	Fraction of P retranslocated from grass leaves at death	fraction	0.01	0.005	0.15
fallrt	Crop	Fall rate (fraction of standing dead which falls each month)	ratio	0.15	0.05	0.25
fligni(1,1)	Crop	Intercept value used in equation to predict lignin content based on annual rainfall for aboveground material	unitless	0.02	0.01	0.2
fligni(1,2)	Crop	Intercept for equation to predict lignin content fraction based on annual rainfall for belowground material	unitless	0.2	0.01	0.2
ppdf(1)	Crop	Optimum temperature for parameterization of a Poisson Density Function curve to simulate temperature effect on plant growth	°C	18	15	25
ppdf(2)	Crop	Maximum temperature for parameterization of a Poisson Density Function curve to simulate temperature effect	°C	35	30	40

(*continued on next page*)

Table A1 (*continued*)

Parameter	Type	Definition	Unit	Initial value	Defined PUR	
					Min	Max
		on plant growth				
ppdf(3)	Crop	Left curve shape for parameterization of a Poisson Density Function curve to simulate temperature effect on growth	unitless	0.9	0.3	1.3
ppdf(4)	Crop	Right curve shape for parameterization of a Poisson Density Function curve to simulate temperature effect on growth	unitless	4.5	0.5	6.5
pramn(1,1)	Crop	Minimum C/N ratio with zero biomass	ratio	20	10	35
pramn(1,2)	Crop	Minimum C/N ratio with biomass greater than or equal to BIOMAX	ratio	30	20	60
pramn(2,1)	Crop	Minimum C/P ratio with zero biomass	ratio	390	200	500
pramn(2,2)	Crop	Minimum C/P ratio with biomass greater than or equal to BIOMAX	ratio	390	300	600
pramx(1,1)	Crop	Maximum C/N ratio with zero biomass	ratio	30	20	80
pramx(1,2)	Crop	Maximum C/N ratio with biomass greater than or equal to BIOMAX	ratio	40	30	120
pramx(2,1)	Crop	Maximum C/P ratio with zero biomass	ratio	440	350	700
pramx(2,2)	Crop	Maximum C/P ratio with biomass greater than or equal to BIOMAX	ratio	440	350	750
prbmn(1,1)	Crop	Intercept parameters for computing minimum C/N ratio for belowground matter as a linear function of annual precipitation	unitless	40	10	60
prbmn(2,1)	Crop	Intercept parameters for computing minimum C/P ratio for belowground matter as a linear function of annual precipitation	unitless	390	190	590
prbmx(1,1)	Crop	Intercept parameters for computing maximum C/N ratio for belowground matter as a linear function of annual precipitation	unitless	50	20	80
prbmx(2,1)	Crop	Intercept parameters for computing maximum C/P ratio for belowground matter as a linear function of annual precipitation	unitless	420	220	620
prdx(1)4_5	Crop	Potential aboveground monthly production as a function of solar radiation	g biomass m-2 month-1	0.35	0.1	0.6
rdrj	Crop	Maximum juvenile fine root death rate at very dry soil conditions (fraction/month)	ratio	0.02	0.01	0.1
rdrm	Crop	Maximum mature fine root death rate at very dry soil conditions (fraction/month)	ratio	0.02	0.01	0.15
rdsrfc	Crop	The fraction of the fine roots that are transferred into the surface litter layer upon root death while the remainder of the roots will go to the soil litter layer	fraction	0.02	0.01	0.15
snfxmx(1)	Crop	Symbiotic N fixation maximum for grass	g N fixed/g C	0.005	0.001	0.1
fdgrem	Grazing	Fraction of standing dead removed by a grazing event	fraction	0.065	0.01	0.12
feclig	Grazing	Lignin content of feces	fraction	0.25	0.15	0.4
flgrem	Grazing	Fraction of live shoots removed by a grazing event	fraction	0.5	0.15	0.75
gfcret	Grazing	Fraction of consumed C which is excreted in feces and urine	fraction	0.3	0.1	0.5
gret(1)	Grazing	Fraction of consumed N which is excreted in feces and urine	fraction	0.8	0.6	0.95
gret(2)	Grazing	Fraction of consumed P which is excreted in feces and urine	fraction	0.95	0.7	0.95
epnfa(1)	Site	Intercept value for determining the effect of annual precipitation on atmospheric N fixation	g N m^{-2} $year^{-1}$	0.21	0.02	0.5
epnfs(1)	Site	Intercept value for determining the effect of annual precipitation on non-symbiotic soil N fixation	g N m^{-2} $year^{-1}$	30	15	45

Table A2
The most sensitive input parameters used in calibration and uncertainty analysis. For each parameter, initial value, defined PUR for Alberta's native grasslands, optimized PUR (aggregated across nine grassland regions) and the percentage of defined PUR covered by the optimized PUR obtained based on the single- (SOC or AGB) and multi-variable (Both) calibration approaches are presented. The level of sensitivity is indicated based on the p-value obtained for each parameter ("**": 0.001 < p-value<0.01; "*": 0.01 < p-values<0.05).

Parameter	Initial value	Defined PUR	Optimized PUR across nine regions			% of defined PUR across regions		
			SOC	AGB	Both	SOC	AGB	Both
aneref(3)*	0.3	0.1–0.8	0.36–0.61	0.33–0.51	0.38–0.48	36	26	14
damr(1,1)*	0.03	0.001–0.2	0.07–0.12	0.05–0.08	0.06–0.8	25	15	10
damrmn(1) **	15	5–20	10.1–13.7	11.4–14.6	11.7–13.8	24	21	14
dec1(1) **	3.9	1–7	3.7–5.5	3.7–5.1	3.9–4.9	30	23	17
dec1(2) **	4.9	2–8	4.8–6.3	5.0–6.0	4.8–5.8	25	17	17
dec2(1) **	14.8	10–20	14.0–16.8	14.2–16.1	14.2–15.7	28	19	15
dec2(2) **	18.5	13.5–23.5	17.3–21.0	18.1–20.6	17.8–19.8	37	25	20
dec3(1) **	6	4–10	6.4–7.5	5.6–7.0	6.4–7.2	18	23	13
dec3(2) **	7.3	4.3–10.3	6.7–7.7	7.2–8.3	6.9–7.7	17	18	13
dec4**	0.0045	0.001–0.03	0.006–0.01	0.01–0.02	0.008–0.013	14	34	17
dec5(1) **	0.2	0.05–0.3	0.14–0.23	0.15–0.21	0.17–0.21	36	24	16
dec5(2) **	0.2	0.05–0.3	0.14–0.20	0.16–0.21	0.16–0.19	24	20	12
deck5**	5	3–7	5.0–5.9	4.1–5.1	4.9–5.6	23	25	18
favail(1)*	0.9	0.1–0.95	0.43–0.64	0.61–0.77	0.51–0.64	25	19	15
favail(4)*	0.2	0.1–0.4	0.21–0.27	0.23–0.26	0.23–0.26	20	10	10
fleach(1)*	0.2	0.1–0.8	0.13–0.15	0.16–0.21	0.18–0.23	3	7	7
fleach(2)*	0.7	0.1–0.8	0.51–0.60	0.43–0.49	0.38–0.45	13	9	10
fwloss(1)*	0.8	0.2–1.4	0.50–0.87	0.61–0.86	0.57–0.77	31	21	17
fwloss(2)*	0.8	0.2–1.4	0.63–0.93	0.67–0.90	0.69–0.89	25	19	17
fwloss(4) *	0.8	0.2–1.2	0.76–0.96	0.77–0.97	0.76–0.96	20	20	20
pcemic(1,1) *	20	15–25	18.7–22.6	18.3–21.6	18.7–20.6	39	33	19
pcemic(2,1) *	10	5–15	8.2–11.7	9.7–12.5	9.2–10.9	35	28	17
peftxa**	0.25	0.1–1	0.42–0.60	0.5–0.6	0.48–0.61	20	11	14
peftxb**	0.75	0.2–0.9	0.45–0.67	0.43–0.54	0.45–0.58	31	16	19
rcestr(1) *	200	50–350	165.6–196	173.7–211	170.6–200.4	10	12	10

Table A2 (*continued*)

Parameter	Initial value	Defined PUR	Optimized PUR across nine regions			% of defined PUR across regions		
			SOC	AGB	Both	SOC	AGB	Both
riint*	0.8	0.6–0.9	0.68–0.88	0.71–0.92	0.79–0.85	67	70	20
teff(1) **	15.4	5–20	13.6–16.4	9.9–12.8	10.6–13.4	19	19	19
teff(2) **	11.75	5–15	8.7–11.4	9.5–11.1	8.8–10.8	27	16	20
teff(3) **	29.7	20–40	29.3–35.3	28.5–33.0	28.9–32.3	30	23	17
teff(4) **	0.031	0.01–0.07	0.036–0.05	0.043–0.05	0.039–0.050	23	12	18
varat11(1,1) *	14	8–30	16.1–20.3	17.3–20.8	16.9–20.1	19	16	15
varat11(2,1) *	3	1–7	3.6–5.3	3.8–4.2	3.6–4.6	28	7	17
varat12(1,1) *	14	10–20	13.9–16.4	14.1–15.9	14.3–16.0	25	18	17
varat12(2,1) *	3	1–9	3.0–4.9	3.9–4.9	3.5–4.9	24	13	18
basetemp(1) **	7	3–10	5.2–7.4	4.8–7.1	4.9–6.7	31	33	26
cfrtcn(1) *	0.6	0.3–1	0.59–0.75	0.51–0.66	0.64–0.71	23	21	10
cfrtcw(1) *	0.6	0.3–1	0.55–0.70	0.59–0.69	0.61–0.71	21	14	14
fligni(1,1) **	0.02	0.01–0.2	0.05–0.08	0.062–0.09	0.061–0.075	16	15	7
fligni(1,2) **	0.2	0.01–0.2	0.131–0.19	0.071–0.10	0.081–0.101	31	15	11
ppdf(1) **	18	15–25	18.7–20.9	18.5–20.6	18.4–20.7	22	21	23
ppdf(2) **	35	30–40	32.8–36.3	33.3–35.7	32.9–35.4	35	24	25
ppdf(3) **	0.9	0.3–1.3	0.70–1.00	0.71–0.90	0.72–0.93	30	19	21
ppdf(4) **	4.5	0.5–6.5	3.5–4.5	3.4–4.6	3.6–4.5	17	22	20
pramn(1,1) *	20	10–35	20.1–25.9	19.8–24.6	23.1–26.1	23	19	12
pramn(1,2) *	30	20–60	35.1–40.0	32.5–40.8	35.0–37.8	12	21	7
pramx(1,1) *	30	20–80	33.6–44.9	38.7–55.3	38.6–45.9	19	28	12
pramx(1,2) *	40	30–120	63.1–73.7	63.7–86.3	62.9–76.7	12	25	15
prbmn(1,1) *	40	10–60	39.3–45.3	35.0–40.1	38.3–41.3	12	10	06
prbmx(1,1) **	50	20–80	39.4–53.7	43.7–53.8	38.9–50.7	24	17	20
prdx(1)4_5**	0.35	0.1–0.6	0.37–0.43	0.36–0.42	0.39–0.43	12	12	08
rdrj*	0.02	0.01–0.1	0.051–0.07	0.046–0.05	0.048–0.066	21	21	20
snfxmx(1) **	0.005	0.001–0.1	0.06–0.08	0.050–0.07	0.058–0.071	20	20	13
flgrem**	0.5	0.15–0.75	0.30–0.64	0.37–0.59	0.48–0.69	57	37	35
gret(1) *	0.8	0.6–0.95	0.75–0.82	0.74–0.84	0.79–0.84	20	29	14
epnfa(1) **	0.21	0.02–0.5	0.18–0.27	0.20–0.25	0.20–0.26	19	10	13
epnfs(1) **	30	15–45	28.2–30.7	28.0–31.0	27.9–30.7	8	10	9

References

Abbaspour, K.C., Yang, J., Maximov, I., Siber, R., Bogner, K., Mieleitner, J., Zobrist, J., Srinivasan, R., 2007. Modeling hydrology and water quality in the pre-Alpine/Alpine Thur watershed using SWAT. J. Hydrol. 333, 413–430.

Abdalla, M., Hastings, A., Chadwick, D.R., Jones, D.L., Evans, C.D., Jones, M.B., Rees, R.M., Smith, P., 2018. Critical review of the impacts of grazing intensity on soil organic carbon storage and other soil quality indicators in extensively managed grasslands. Agric. Ecosyst. Environ. 253, 62–81.

ABMI (Alberta Biodiversity Monitoring Institute), 2012. ABMI Wall-to-Wall Land Cover Map Circa 2010, Version 1.0. Alberta Biodiversity Monitoring Institute, Alberta, Canada https://abmi.ca/home/data-analytics/da-top/da-product-overview/GIS-Land-Surface/Land-Cover.html.

ABMI (Alberta Biodiversity Monitoring Institute), 2016a. Terrestrial Field Data Collection Protocols (Abridged Version; 2014-03-21). Alberta Biodiversity Monitoring Institute, Alberta, Canada http://www.abmi.ca/home/publications/1-50/46.html.

ABMI (Alberta Biodiversity Monitoring Institute), 2016b. 2014 Human Footprint Map Layer Version 1.1- Metadata. Alberta Biodiversity Monitoring Institute, Alberta, Canada http://abmi.ca/home/data-analytics/da-top/da-product-overview/GIS-Land-Surface/HF-inventory.html.

Adhikari, K., Hartemink, A.E., 2016. Linking soils to ecosystem services – a global review. Geoderma 262, 101–111.

AESRD (Alberta Environment & Sustainable Resource Development), 2015. 2014 Range Reference Area Report for the Grasslands. AESRD Range Resource Management Program, Alberta, Canada (unpublished report).

Alberta Environment, 2006. 2004 Acid Deposition Assessment for Alberta. A Report of the Acid Deposition Assessment Group. Prepared by. WBK & Associates Inc, Edmonton, Canada (93 pp).

Álvaro-Fuentes, J., Easter, M., Paustian, K., 2012. Climate change effects on organic carbon storage in agricultural soils of northeastern Spain. Agric. Ecosyst. Environ. 155, 87–94.

ASIC (Alberta Soil Information Centre), 2001. In: Brierley, J.A., Martin, T.C., Spiess, D.J. (Eds.), AGRASID 3.0: Agricultural Region of Alberta Soil Inventory Database (Version 3.0). Agriculture and Agri-Food Canada, Research Branch; Alberta Agriculture, Food and Rural Development, Conservation and Development Branch http://www1.agric.gov.ab.ca/$department/deptdocs.nsf/all/sag3253?opendocument.

Blair, J., Nippert, J., Briggs, J., 2014. Grassland ecology. In: Jonson, R.K. (Ed.), Ecology and the Environment, pp. 389–423.

Brandani, C.B., Abbruzzini, T.F., Williams, S., Easter, M., Pellegrino Cerri, C.E., Paustian, K., 2015. Simulation of management and soil interactions impacting SOC dynamics in sugarcane using the CENTURY model. GCB Bioenergy 7, 646–657.

Brown, J., Angerer, J., Salley, S.W., Blaisdell, R., Stuth, J.W., 2010. Improving estimates of rangeland carbon sequestration potential in the US south-west. Rangel. Ecol. Manag. 63, 147–154.

Campbell, E.E., Paustian, K., 2015. Current developments in soil organic matter modeling and the expansion of model applications: a review. Environ. Res. Lett. 10, 123004.

Cerri, C.E.P., Easter, M., Paustian, K., Killian, K., Coleman, K., Bernoux, M., Falloon, P., Powlson, D.S., Batjes, N., Milne, E., Cerri, C.C., 2007. Simulating SOC changes in 11 land use change chronosequences from the Brazilian Amazon with RothC and CENTURY models. Agric. Ecosyst. Environ. 122, 46–57.

Chang, X., Bao, X., Wang, S., Wilkes, A., Erdenetsetseg, B., Baival, B., Avaadorj, D., Maisaikhan, T., Damdinsuren, B., 2015. Simulating effects of grazing on soil organic carbon stocks in Mongolian grasslands. Agric. Ecosyst. Environ. 212, 278–284.

Chetner, S., the Agroclimatic Atlas Working Group, 2003. Agroclimatic Atlas of Alberta, 1971 to 2000. Alberta Agriculture, Food and Rural Development, Agdex 071–1. Edmonton, Alberta.

Cleveland, C.C., Townsend, A.R., Schimel, D.S., Fisher, H., Howarth, R.W., Hedin, L.O., Perakis, S.S., Latty, E.F., von Fischer, J.C., Elseroad, A., Wasson, M., 1999. Global patterns of terrestrial biological nitrogen (N2) fixation in natural ecosystems. Glob. Biogeochem. Cycles 13, 623–645.

Cord, A.F., Brauman, K.A., Chaplin-Kramer, R., Huth, A., Ziv, G., Seppelt, R., 2017. Priorities to advance monitoring of ecosystem services using Earth observation. Trends Ecol. Evol. 32, 416–428.

Cuddington, K., Fortin, M.J., Gerber, L.R., Hastings, A., Liebhold, A., O'Connor, M., Ray, C., 2013. Process-based models are required to manage ecological systems in a changing world. Ecosphere 4, 1–12.

Daily, G.C., Polasky, S., Goldstein, J., Kareiva, P.M., Mooney, H.A., Pejchar, L., Ricketts, T.H., Salzman, J., Shallenberger, R., 2009. Ecosystem services in decision making: time to deliver. Front. Ecol. Environ. 7, 21–28.

de Gruijter, J.J., McBratney, A.B., Minasny, B., Wheeler, I., Malone, B.P., Stockmann, U., 2016. Farm-scale soil carbon auditing. Geoderma 265, 120–130.

Didan, K., 2015. MOD13Q1 MODIS/Terra Vegetation Indices 16-Day L3 Global 250m SIN Grid V006, Distributed by NASA EOSDIS Land Processes DAAC. https://doi.org/10.5067/MODIS/MOD13Q1.006.

Dimassi, B., Guenet, B., Saby, N.P.A., Munoz, F., Bardy, M., Millet, F., Martin, M.P., 2018. The impacts of CENTURY model initialization scenarios on soil organic carbon dynamics simulation in French long-term experiments. Geoderma 311, 25–36.

Faramarzi, M., Srinivasan, R., Iravani, M., Bladon, K.D., Abbaspour, K.C., Zehnder, A.J.B., Goss, G.G., 2015. Setting up a hydrological model of Alberta: data discrimination analyses prior to calibration. Environ. Model Softw. 74, 48–65.

Faramarzi, M., Abbaspour, K.C., Adamowicz, W.L., Lu, W., Fennell, J., Zehnder, A.J.B., Goss, G.G., 2017. Uncertainty based assessment of dynamic freshwater scarcity in semi-arid watersheds of Alberta, Canada. J. Hydrol. Reg. Stud. 9, 48–68.

Feng, X.M., Zhao, Y.S., 2011. Grazing intensity monitoring in Northern China steppe: integrating CENTURY model and MODIS data. Ecol. Indic. 11, 175–182.

Gibson, D.J., 2009. Grasses and Grassland Ecology. Oxford University Press, Oxford, UK.

Gilmanov, T., Parton, W., Ojima, D., 1997. Testing the 'CENTURY' ecosystem level model on datasets from eight grassland sites in the former USSR representing a wide climatic/soil gradient. Ecol. Model. 96, 191–210.
Grigera, G., Oesterheld, M., Pacin, F., 2007. Monitoring forage production for farmers' decision making. Agric. Syst. 94, 637–648.
Downing, D.J., Pettapiece, W.W., 2006. Natural Regions and Subregions of Alberta. Natural Regions Committee, Government of Alberta Pub. No. T/852.
Gu, Y., Wylie, B.K., 2015. Developing a 30-m grassland productivity estimation map for central Nebraska using 250-m MODIS and 30-m Landsat-8 observations. Remote Sens. Environ. 171, 291–298.
Gu, Y., Wylie, B.K., Bliss, N.B., 2013. Mapping grassland productivity with 250-m eMODIS NDVI and SSURGO database over the Greater Platte River Basin, USA. Ecol. Indic. 24, 31–36.
Gupta, H.V., Sorooshian, S., Yapo, P.O., 1998. Toward improved calibration of hydrologic models: multiple and noncommensurable measures of information. Water Resour. Res. 34, 751–763.
Havstad, K.M., Peters, D.P.C., Skaggs, R., Brown, J., Bestelmeyer, B., Fredrickson, E., Herrick, J., Wright, J., 2007. Ecological services to and from rangelands of the United States. Ecol. Econ. 64, 261–268.
Hewins, D.B., Lyseng, M.P., Schoderbek, D.F., Alexander, M., Willms, W.D., Carlyle, C.N., Chang, S.X., Bork, E.W., 2018. Grazing and climate effects on soil organic carbon concentration in northern grasslands. Sci. Rep. 8, 1336.
Holland, E.A., Parton, W.J., Detling, J.K., Coppock, D.L., 1992. Physiological responses of plant populations to herbivory and their consequences for ecosystem nutrient flow. Am. Nat. 140, 685–706.
Hou, Y., Burkhard, B., Müller, F., 2013. Uncertainties in landscape analysis and ecosystem service assessment. J. Environ. Manag. 127, 117–131.
Howe, C., Suich, H., Vira, B., Mace, G.M., 2014. Creating win-wins from trade-offs? Ecosystem services for human well-being: a meta-analysis of ecosystem service trade-offs and synergies in the real world. Glob. Environ. Chang. 28, 263–275.
Hungate, B.A., Barbier, E.B., Ando, A.W., Marks, S.P., Reich, P.B., van Gestel, N., Tilman, D., Knops, J.M.H., Hooper, D.U., Butterfield, B.J., Cardinale, B.J., 2017. The economic value of grassland species for carbon storage. Sci. Adv. 3, e1601880.
Jack, K., Kousky, C., Sims, K., 2008. Designing payments for ecosystem services: lessons from previous experience with incentive-based mechanisms. Proc. Natl. Acad. Sci. 105, 9465–9470.
Jellinek, S., Wilson, K.A., Hagger, V., Mumaw, L., Cooke, B., Guerrero, A.M., Erickson, T.E., Zamin, T., Waryszak, P., Standish, R.J., 2019. Integrating diverse social and ecological motivations to achieve landscape restoration. J. Appl. Ecol. 56, 246–252.
Jönsson, P., Eklundh, L., 2004. TIMESAT—A program for analyzing time-series of satellite sensor data. Comput. Geosci. 30, 833–845.
Kariyeva, J., van Leeuwen, W.J.D., 2012. Phenological dynamics of irrigated and natural drylands in Central Asia before and after the USSR collapse. Agric. Ecosyst. Environ. 162, 77–89.
Kwon, H., Ugarte, C.M., Ogle, S.M., Williams, S.A., Wander, M.M., 2017. Use of inverse modeling to evaluate CENTURY-predictions for soil carbon sequestration in US rainfed corn production systems. PLoS One 12, e0172861.
Lapp, S.L., St. Jacques, J.M., Sauchyn, D.J., Vanstone, J.R., 2013. Forcing of hydroclimatic variability in the northwestern Great Plains since AD 1406. Quat. Int. 310, 47–61.
Li, W., Li, X., Zhao, Y., Zheng, S., Bai, Y., 2018. Ecosystem structure, functioning and stability under climate change and grazing in grasslands: current status and future prospects. Curr. Opin. Environ. Sustain. 33, 124–135.
Liu, S., Cheng, F., Dong, S., Zhao, H.D., Hou, X.Y., Wu, X., 2017. Spatiotemporal dynamics of grassland aboveground biomass on the Qinghai-Tibet Plateau based on validated MODIS NDVI. Sci. Rep. 7, 1–8.
Lopez-Marsico, L., Altesor, A., Oyarzabal, M., Baldassini, P., Paruelo, J.M., 2015. Grazing increases below-ground biomass and net primary production in a temperate grassland. Plant Soil 392, 155–162.
Lugato, E., Panagos, P., Bampa, F., Jones, A., Montanarella, L., 2014. A new baseline of organic carbon stock in European agricultural soils using a modeling approach. Glob. Chang. Biol. 20, 313–326.
Meersmans, J., Martin, M.P., Lacarce, E., Orton, T.G., De Baets, S., Gourrat, M., Saby, N.P.A., Wetterlind, J., Bispo, A., Quine, T.A., Arrouays, D., 2013. Estimation of soil carbon input in France: an inverse modeling approach. Pedosphere 23, 422–436.
Metherell, A.K., Harding, L.A., Cole, C.V., Parton, W.J., 1993. CENTURY Soil Organic Matter Model Environment, Agroecosystem Version 4.0. GPSR Tech. Report No. 4. United States Department of Agriculture, Agricultural Research Service, Fort Collins, CO, USA.
Murphy, K.L., Burke, I.C., Vinton, M.A., Lauenroth, W.K., Aguiar, M.R., Wedin, D.A., Virginia, R.A., Lowe, P., 2002. Regional analysis of litter quality in the central grassland region of North America. J. Veg. Sci. 13, 395–402.
Necpálová, M., Anex, R.P., Fienen, M.N., Del Grosso, S.J., Castellano, M.J., Sawyer, J.E., Iqbal, J., Pantoja, J.L., Barker, D.W., 2015. Understanding the DayCent model: calibration, sensitivity, and identifiability through inverse modeling. Environ. Model Softw. 66, 110–130.
Niquil, N., Saint-Béat, B., Johnson, G.A., Soetaert, K., van Oevelen, D., Bacher, C., Vézina, A.F., 2011. Inverse modeling in modern ecology and application to coastal ecosystems. In: Wolanski, E., McLusky, D.S. (Eds.), Treatise on Estuarine and Coastal Science. Vol 9, pp. 115–133.
Oelbermann, M., Voroney, R.P., 2011. An evaluation of the century model to predict soil organic carbon: examples from Costa Rica and Canada. Agrofor. Syst. 82, 37–50.
Ogle, S.M., Breidt, F.J., Easter, M., Williams, S., Paustian, K., 2007. An empirically based approach for estimating uncertainty associated with modeling carbon sequestration in soils. Ecol. Model. 205, 453–463.
Ogle, S.M., Breidt, F.J., Easter, M., Williams, S., Killian, K., Paustian, K., 2010. Scale and uncertainty in modeled soil organic carbon stock changes for US croplands using a process-based model. Glob. Chang. Biol. 16, 810–822.
Parton, W.J., Schimel, D.S., Cole, C.V., Ojima, D.S., 1987. Analysis of factors controlling soil organic matter levels in Great Plains grasslands. Soil Sci. Soc. Am. J. 51, 1173–1179.
Parton, W.J., Stewart, J.W.B., Cole, C.V., 1988. Dynamics of C, N, P and S. in grassland soils: a model. Biogeochemistry 5, 109–131.
Parton, W.J., Cole, C.V., Stewart, J.W.B., Ojima, D.S., Schimel, D.S., 1989. Simulating regional patterns of soil C, N, and P dynamics in the US central grasslands region. In: Clarholm, M., Bergstrom, L. (Eds.), Ecology of Arable Lands. Kluwer Academic Publishers, Amsterdam, Netherlands, pp. 99–108.
Parton, W.J., Scurlock, J.M.O., Ojima, D.S., Gilmanov, T.G., Scholes, R.J., Schimel, D., Kirchner, T., Menaut, J., Seastedt, T., Moya, E., 1993. Observations and modeling of biomass and soil organic matter dynamics for the grassland biome worldwide. Glob. Biogeochem. Cycles 7, 785–809.
Parton, W.J., Scurlock, J.M.O., Ojima, D.S., Schimel, D.S., Hall, D.O., Scopegram Group Members, 1995. Impact of climate change on grassland production and soil carbon worldwide. Glob. Chang. Biol. 1, 13–22.
Parton, W., Tappan, G., Ojima, D., Tschakert, P., 2004. Ecological impact of historical and future land-use patterns in Senegal. J. Arid Environ. 59, 605–623.
R Development Core Team, 2017. R: A Language and Environment for Statistical Computing. R Foundation for Statistical Computing, Vienna http://www.R-project.org.
Rafique, R., Fienen, M.N., Parkin, T.B., Anex, R.P., 2013. Nitrous oxide emissions from cropland: a procedure for calibrating the DAYCENT biogeochemical model using inverse modeling. Water Air Soil Pollut. 224, 1–15.
Rafique, R., Kumar, S., Luo, Y., Kiely, G., Asrar, G.R., 2015. An algorithmic calibration approach to identify globally optimal parameters for constraining the DayCent model. Ecol. Model. 297, 196–200.
Sándor, R., Ehrhardt, F., Brilli, L., Carozzi, M., Recous, S., Smith, P., Snow, V., Soussana, J.F., Dorich, C.D., Fuchs, K., Fitton, N., Gongadze, K., Klumpp, K., Liebig, M., Martin, R., Merbold, L., Newton, P.C.D., Rees, R.M., Rolinski, S., Bellocchi, G., 2018. The use of biogeochemical models to evaluate mitigation of greenhouse gas emissions from managed grasslands. Sci. Total Environ. 642, 292–306.
Schimel, D.S., Braswell, B.H., Holland, E.A., McKeown, R., Ojima, D.S., Painter, T.H., Parton, W.J., Townsend, A.R., 1994. Climatic, edaphic, and biotic controls over storage and turnover of carbon in soils. Glob. Biogeochem. Cycles 8, 279–293.
Schulp, C.J.E., Burkhard, B., Maes, J., Van Vliet, J., Verburg, P.H., 2014. Uncertainties in ecosystem service maps: a comparison on the European scale. PLoS One 9, e109643.
Smith, P., Smith, J.U., Powlson, D.S., McGill, W.B., Arah, J.R.M., Chertov, O.G., Coleman, K., Franko, U., Frolking, S., Jenkinson, D.S., Jensen, L.S., Kelly, R.H., Klein-Gunnewiek, H., Komarov, A.S., Li, C., Molina, J.A.E., Mueller, T., Parton, W.J., Thornley, J.H.M., Whitmore, A.P., 1997a. A comparison of the performance of nine soil organic matter models using data sets from seven long-term experiments. Geoderma 81, 153–225.
Smith, W.N., Rochett, P., Monreal, C., Desjardins, R.L., Pattey, E., Jaques, A., 1997b. The rate of carbon change in agricultural soils in Canada at the landscape level. Can. J. Soil Sci. 77, 219–229.
Smith, W.N., Grant, B.B., Desjardins, R.L., Hutchinson, Qian, Gameda, B.J., 2009. Potential impact of climate change on carbon in agricultural soils in Canada: 2000-2099. Clim. Chang. 93, 319–333.
Stamp, R.M., Warnell, D., 2008. Alberta. The Canadian Encyclopedia. Historica Foundation of Canada. http://www.thecanadianencyclopedia.com/en/article/alberta/, Accessed date: 1 October 2008.
Van den Bygaart, A.J., McConkey, B.G., Angers, D.A., Smith, W., de Gooijer, H., Bentham, M., Martin, T., 2008. Soil carbon change factors for the Canadian agriculture national greenhouse gas inventory. Can. J. Soil Sci. 88, 671–680.
Wang, Y., Zhou, G., Jia, B., 2008. Modeling SOC and NPP responses of meadow steppe to different grazing intensities in Northeast China. Ecol. Model. 217, 72–78.
Wang, T., Hamann, A., Spittlehouse, D.L., Murdock, T.Q., 2012. ClimateWNA – high-resolution spatial climate data for western North America. J. Appl. Meteorol. Climatol. 51, 16–29.
Wang, F., Mladenoff, D.J., Forrester, J.A., Keough, C., Parton, W.J., 2013. Global sensitivity analysis of a modified CENTURY model for simulating impacts of harvesting fine woody biomass for bioenergy. Ecol. Model. 259, 16–23.
Wang, X., VandenBygaart, A.J., McConkey, B.C., 2014. Land management history of Canadian grasslands and the impact on soil carbon storage. Rangel. Ecol. Manag. 67, 333–343.
Wiesmeier, M., Urbanski, L., Hobley, E., Lang, B., von Lützow, M., Marin-Spiotta, E., van Wesemael, B., Rabot, E., Ließ, M., Garcia-Franco, N., Wollschläger, U., Vogel, H.J., Kögel-Knabner, I., 2019. Soil organic carbon storage as a key function of soils - a review of drivers and indicators at various scales. Geoderma 333, 149–162.
Xiong, X., Grunwald, S., Myers, D.B., Kim, J., Harris, W.G., Bliznyuk, N., 2015. Assessing uncertainty in soil organic carbon modeling across a highly heterogeneous landscape. Geoderma 251, 105–116.